Photochemical Metal Organic Deposition (PMOD)

of Metal Oxide Films and Multilayer Films

by

Hui Jian (Juli) Zhu

B. Sc., China Textile University, 1985

THESIS SUBMITTED IN PARTIAL FULFILLMENT OF

THE REQUIREMENTS FOR THE DEGREE OF MASTER OF SCIENCE

in the Department

of

Chemistry

© Hui Jian (Juli) Zhu 2001

Simon Fraser University

March 2001

The author has granted a non-exclusive licence allowing the National Library of Canada to reproduce, loan, distribute or sell copies of this thesis in microform, paper or electronic formats.

L'auteur a accordé une licence non exclusive permettant à la Bibliothèque nationale du Canada de reproduire, prêter, distribuer ou vendre des copies de cette thèse sous la forme de microfiche/film, de reproduction sur papier ou sur format électronique.

The author retains ownership of the copyright in this thesis. Neither the thesis nor substantial extracts from it may be printed or otherwise reproduced without the author's permission.

L'auteur conserve la propriété du droit d'auteur qui protège cette thèse. Ni la thèse ni des extraits substantiels de celle-ci ne doivent être imprimés ou autrement reproduits sans son autorisation.

0-612-61617-7

Canada

Abstract

This thesis will describe the use of Photochemical Metal Organic Deposition (PMOD) to fabricate single layer metal oxide films. The thin films of precursors were prepared by a spin coating technique. The precursor films were exposed to UV light and photochemically produced titanium oxide and manganese oxide films.

The photochemical reactions of $Ti(i-prop)_2(acac)_2$ and $Mn(O_2CCH(C_2H_5)C_4H_9)_2$ precursor films were monitored by Fourier Transform Infrared Spectroscopy. The volatile products from the photolysis of these precursors were identified by Mass spectroscopy. The photoproduced films were characterized by Auger electron spectroscopy and x-ray powder diffraction. Finally, mechanisms which accounted for the photochemical reactions of these precursors were proposed.

This thesis will also describe our first attempts at applying PMOD (Photochemical Metal Organic Deposition) to fabricate alternating multilayer thin films. The components we chose to fabricate multilayer samples were titanium oxide and manganese oxide. The prepared samples were investigated by means of X-ray diffraction. The bilayer thickness of multilayer samples were 4 ~ 10 nm. The total film thickness of the samples were 40 ~ 200 nm.

The as deposited multilayer samples were amorphous layered films. After a sample was heated at 300°C, it was still amorphous but evidence which indicated a layered structure was lost. After the sample was heated at 700°C, a solid solution $Mn_pTi_{2-p}O_3$ with α-Mn_2O_3 structure and rutile was formed.

Dedication

To my parents with lots of love

Acknowledgements

It is with much pleasure that I acknowledge the valuable support and guidance of my senior supervisor Dr. Ross H. Hill throughout my graduate school experience.

My special thanks go to Vice President Dr. Sharon L. Blair of Lightyear Technologies Inc. without whose support my goal could not have been accomplished.

A thank you also goes to my labmates for their help and friendship. Special thanks are given to Mr. Juan Pablo Bravo, Ms. Guizhi Li and Mr. Simon Law for their help of experiments. I would also like to thank Mr. Greg L. Owen, for running MS samples and Dr. B. Heinrich for allow us using AES.

I sincerely thank my husband Zuwei Gu for his understanding and encouragement.

Finally I wish to acknowledge the generous financial support from Dr. Ross H. Hill, the Chemistry Department and Simon Fraser University.

Table of Contents

Chapter 3 Preparation and characterization of manganese oxide films

Chapter 4 Fabrication of titanium oxide and manganese oxide multilayered films

List of Figures

List of Tables

List of Abbreviations

i-prop:	isopropoxide ($OCH(CH_3)_2$)
acac:	acetylacetonate ($CH_3COCHCOCH_3$)[-]
PMOD:	photochemical metal organic deposition
MS:	Mass Spectrometry
FTIR:	Fourier transform infrared
IR:	infrared
XRD:	X-ray diffraction
AES:	Auger electron spectroscopy
M:	metal
L:	ligand
LMCT:	ligand to metal charge transfer
2θ:	diffraction angle
UV:	ultraviolet
Si:	silicon
λ:	wavelength
MSD:	magnetron sputter deposition
PVD:	physical vapor deposition
CVD:	chemical vapor deposition

Chapter 1 Introduction

Multilayer thin films periodic in one dimension in composition create new materials

having microstructures not found in nature. By alternating deposition of two compounds,

multilayer thin films can be fabricated. Several deposition techniques have been used to

prepare these materials.[1-4]

This thesis describes the development of photochemical metal organic deposition

(PMOD) to produce multilayer thin films. The approach provides a simple route to

multilayer thin films. In order to provide background for understanding the project, this

chapter is organized into four sections. Section 1.1 will introduce photochemical metal

organic deposition (PMOD). This is a method developed in our laboratory to prepare

single layer films. Section 1.2 will propose use of PMOD to prepare multilayer films.

This is followed by introduction of surface analysis method, X-ray powder diffraction

and Auger electron spectroscopy. Finally, section 1.4 will provide the organization of the

thesis.

1.1 Photochemical metal organic deposition (PMOD)

Photochemical metal organic deposition (PMOD) has been used to deposit many

materials. These materials include the metal oxides of Cu, Co, Ni, Pt[5] as well as the

mixed metal oxides such as $(Pb_{0.5}Zr_{0.5})TiO_3$, $(Ba_{0.5}Sr_{0.5})TiO_3$.[6, 7] The process of PMOD is

outlined in figure 1-1
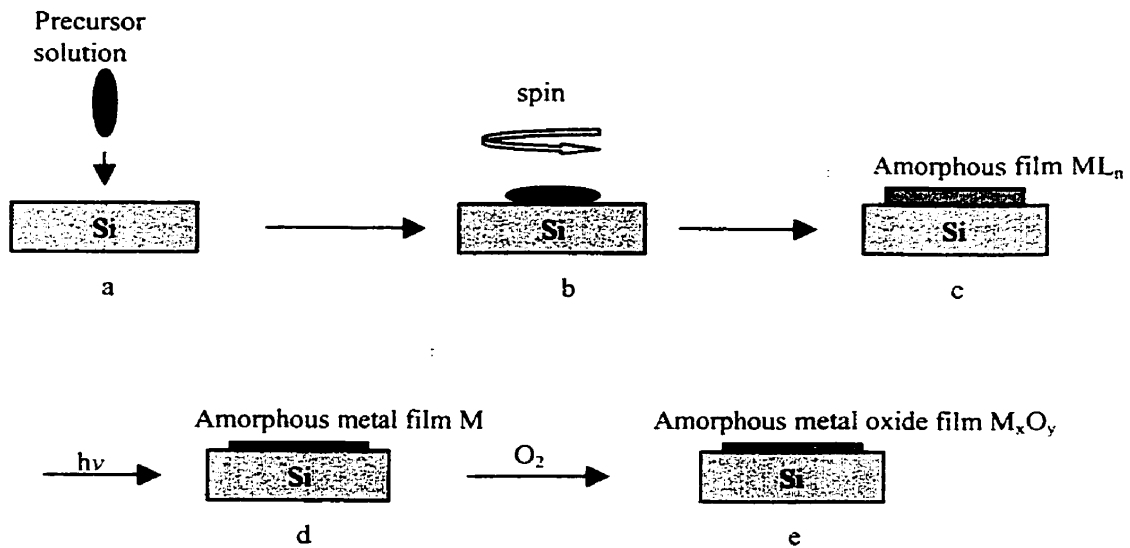
Figure 1-1 The PMOD of a metal oxide film

A precursor solution which contains the starting material ML_n (M is a metal and L_n is the ligand) in a volatile solvent is first prepared. The deposition process begins by dispensing this precursor solution on a stationary silicon substrate (figure 1-1a). The substrate is then accelerated to a spin speed (normally between 1000-3000rpm, figure 1-1b). The solvent evaporates leaving an amorphous film of ML_n on the substrate (figure 1-1c). The precursor film is then exposed to ultra-violet radiation. Upon irradiation, volatile ligands are ejected from the metal center leaving an amorphous metal film on the substrate (figure 1-1d). Reaction of the metal center with oxygen in air leads to the production of amorphous metal oxide film, M_xO_y (figure 1-1e).

2

It is important to point out that step d and step e are idealized representation. Normally, in the presence of an oxygen source, M_xO_y is formed while the photolysis is occurring. In this case the amorphous metal film is not formed.

There are certain criteria for an ideal precursor. The PMOD is a photochemical reaction, so the precursor has to be photosensitive. When dissolved in a solvent, it must form an amorphous film upon spin coating on the substrate. A crystalline film is not ideal because the strong intermolecular forces between molecules lead to recombination of the primary photochemical products. This recombination results in a low reaction quantum yield. The precursor must also be nonvolatile and thermally stable. This makes it possible to carry out the process at room temperature under atmospheric pressure.

1.2 Proposed use of PMOD to prepare multilayer films

The goal of this thesis is to use photochemical metal organic deposition (PMOD) to fabricate multilayer films. The fabrication procedures of multilayer films by PMOD are shown in figure 1-2.

Two metal organic compounds MaLn and MbLm are starting materials (Ma, Mb are two different metals and Ln, Lm are two different ligands). The precursor solutions are prepared by mixing starting materials with solvents. The deposition process begins by dispensing MaLn precursor solution on a stationary silicon substrate (figure 1-2a). The substrate is then accelerated to a spin speed (figure 1-2b). The solvent evaporates
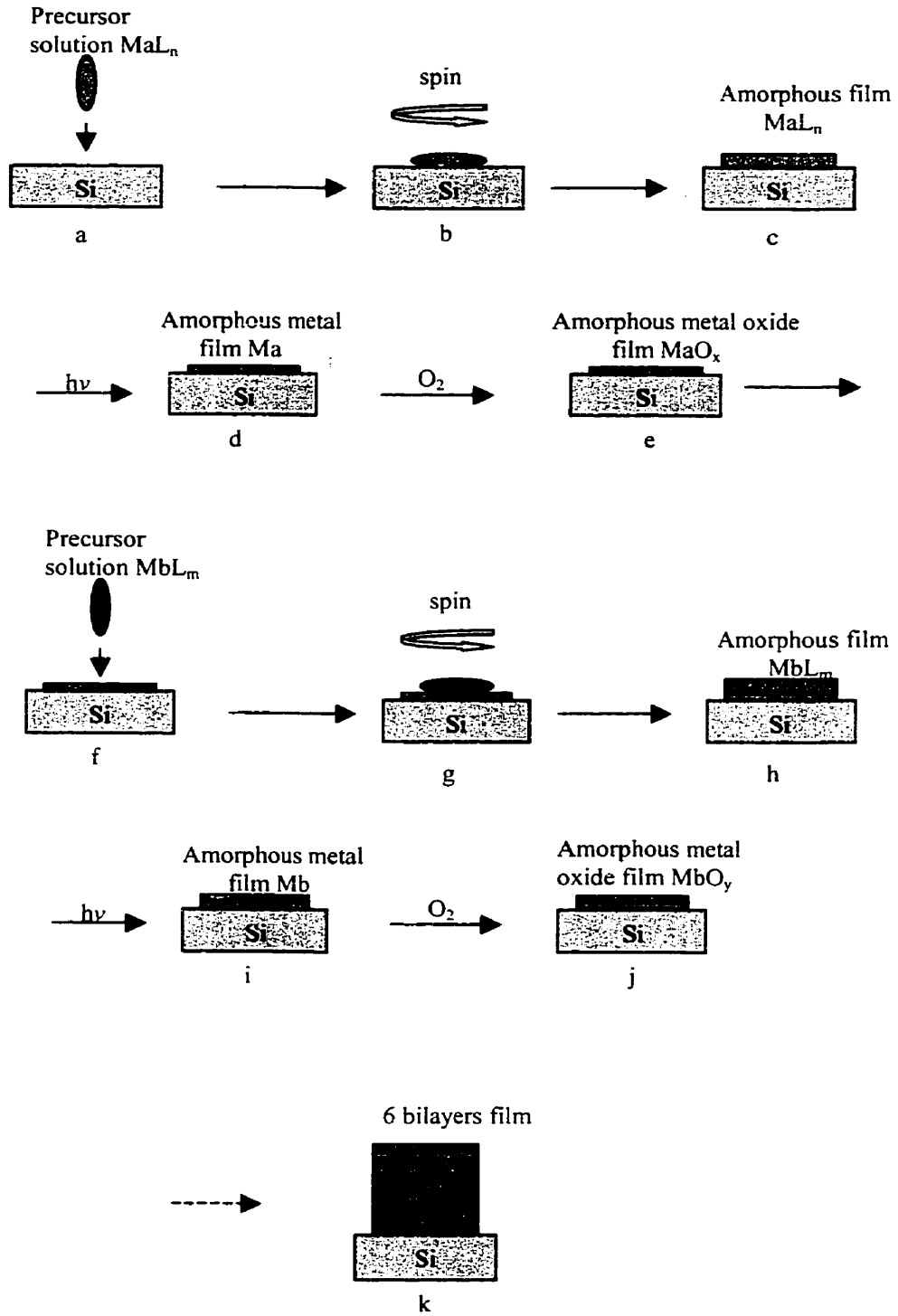
Figure 1-2 The fabrication procedures of multilayer films by PMOD

leaving an amorphous MaLn film on the substrate (figure 1-2c). The precursor film is

irradiated using UV light until all the ligands have been ejected. An amorphous Ma film

is formed on the substrate (figure 1-2d). The Ma film reacts with the oxygen in air

leading to the production of a MaO_x film (figure 1-2e). The MbLm precursor solution is

then dispensed on the stationary MaO_x layer (figure 1-2f). The substrate is then

accelerated to a spin speed (figure 1-2g). The solvent evaporates leaving an amorphous

MbLm film on the substrate (figure 1-2h). The film is then irradiated under UV light

until all the ligands have been ejected. This result in the formation of amorphous Mb

film on the MaO_x layer (figure 1-2i). The Mb film reacts with the oxygen in air leading

to the production of a MbO_y film on the MaO_x layer (figure 1-2j). The procedures are

repeated by repeating the entire process to build the multilayer material (figure 1-2k). As

mentioned earlier, in the presence of an oxygen source the metal oxides are formed while

the photolysis is occurring. In this case the amorphous metal films Ma, Mb are not

formed.

There are many existing techniques for the deposition of multilayer films. In order to

explain why we are developing an other method to deposit multilayer films, we need to

review existing methods. This will allow us to contrast those methods with the proposed

method.

Several deposition methods have been investigated in regard to multilayer film

deposition such as: dual magnetron sputter deposition[1] (MSD), sol-gel coating[2],

ultrahigh-vacuum physical vapor deposition[3] (PVD) and chemical vapor deposition[4]

(CVD) etc. However, some of these processes, for example CVD, sol-gel coating,

operate at high temperatures and others require high vacuum systems (MSD, PVD).

The disadvantages of high temperature processes are the possibility of damage to the films that were previously deposited on the substrate and interdiffusion of the layered films. The disadvantages of the high vacuum processes are the high cost of the equipment and the time consumed in achieving the vacuum. As a result, the development of new processes to fabricate multilayer films is important.

The new process we introduced above (PMOD) has some advantages. First, the reaction is carried out at room temperature. Second, reaction does not require a sophisticated vacuum chamber as it can be carried out under atmospheric pressure.

In this contribution, the products of the photochemical reaction are characterized by surface analysis techniques. They include mass spectrometry, Auger electron spectroscopy, high and low angle x-ray powder diffraction (XRD). An outline of these techniques will be described in section 1.3.

1.3 Thin film analysis methods

1.3.1 X-ray powder diffraction

In this study, X-ray powder diffraction was used to identify the crystal structure of thin films and measure the thickness of multilayer films. X-ray powder diffraction has been long used for the structural identification of crystals. X-ray diffraction also is a

powerful technique for analysis of multilayer structures. It is a non-destructive technique. The analysis can be done while the sample is on the substrate.
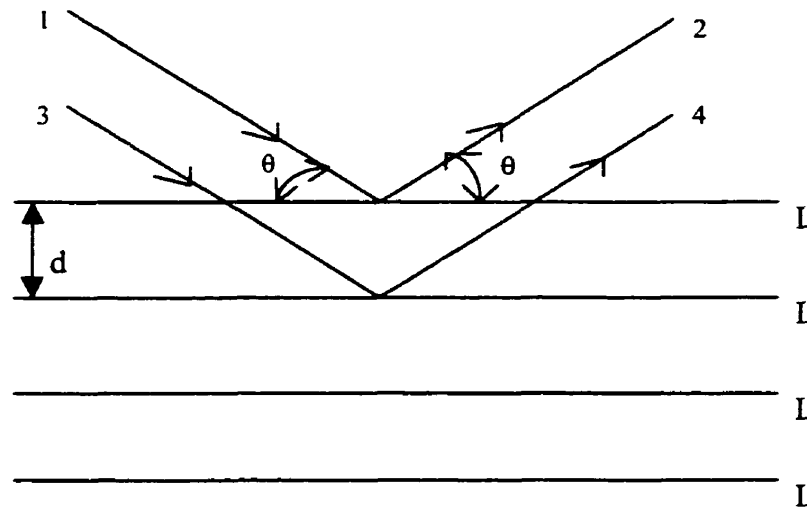
Figure 1-3 X-ray diffraction from a sample

Figure 1-3 illustrates the Bragg condition for the reflection of X-rays by a sample. The Bragg condition is satisfied when diffracted X-rays are in phase and constructively interfere. In figure 1-3, L are adjacent planes within a sample. Lines 1 and 3 represent two incident X-ray beams. Lines 2 and 4 represent reflected beams from adjacent planes within the sample. The perpendicular distance between adjacent planes is given as d. θ is the angle between incident beam and each plane parallel of the sample, i.e. the Bragg angle.

The difference in the path length traveled by the two beams is $2d\sin\theta$. If this difference is equal to an integral number, n, of X-ray wavelengths, λ, then the reflected

beams 3 and 4 are in phase. The in phase relation results in the observation of diffraction. When this is true, the Bragg condition is satisfied.

$$n\lambda = 2d\sin\theta \qquad 1\text{-}1$$

Equation 1-1, which describes this condition, is known as the Bragg equation. The Bragg equation can be rewritten as Equation 1-2.

$$d = n\lambda/2\sin\theta \qquad 1\text{-}2$$

From the value of θ and the X-ray wavelength λ, we can calculate the distance of the perpendicular planes of the sample, d. The X-ray we used is from Cu K_α irradiation. The wavelength from its irradiation is 1.54 Å.

When the adjacent planes are within the crystal, the calculated d is the space between the crystal planes.

For a multilayer sample, the adjacent planes can be layers of components A and B. The Bragg condition for the reflection of X-rays is illustrated in figure 1-4. From the equation 1-2, we can also calculate d, which is the bilayer thickness of multilayer sample. The bilayer thickness of the multilayer samples studied here are approximately 4~10 nm, so the diffraction angle 2θ is in the range between 0.9° to 5°.
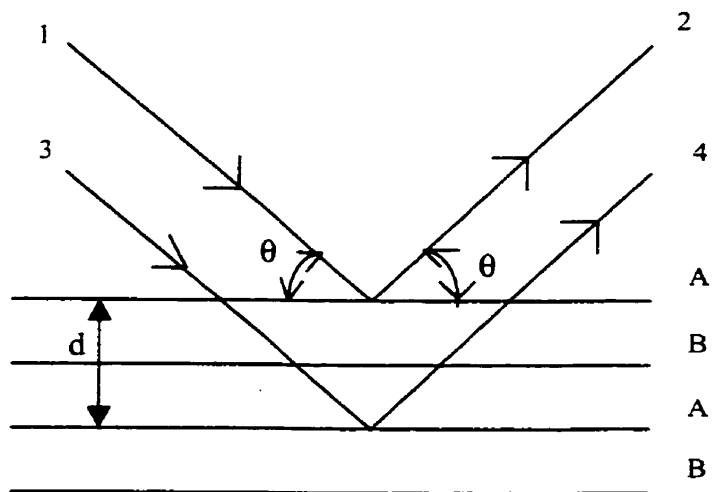
Figure 1-4 X-ray diffraction on a multilayer sample

1.3.2 Auger electron spectroscopy

Auger electron spectroscopy (AES) is a method used to determine elemental composition of surfaces. The process of Auger electron generation is illustrated in Figure 1-5.[8]
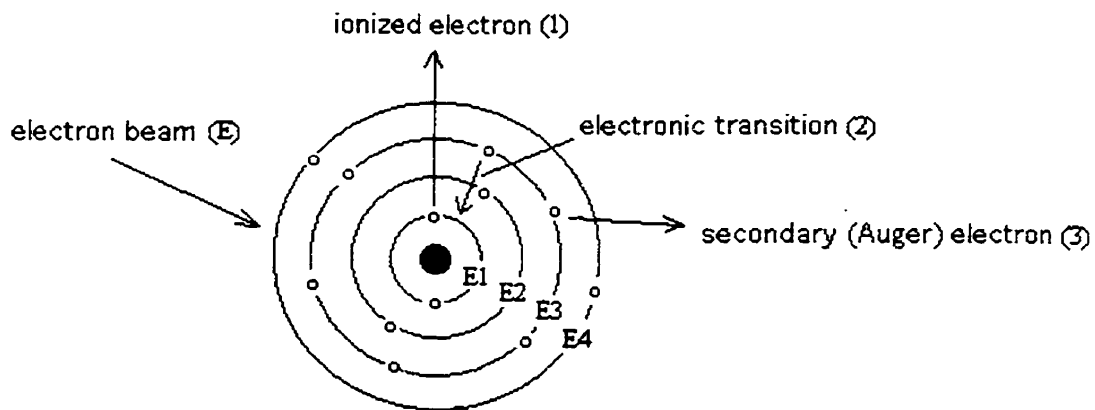
(E1, E2, E3, E4 represent energy levels in an atom)

Figure 1-5 The process of Auger electron generation

When a sample is bombarded with an electron beam (E), a core level electron (1) is ejected from the atom leaving a vacancy (figure 1-5). An electron from higher energy level (2) fills the vacancy. The energy (E1-E3) resulting from this transition can be transferred to another electron (3) in the same atom, which is then ejected. Such secondary ionized electrons are Auger electrons. The kinetic energy of the Auger electron, E_A, is given by equation 1-3. The Auger electron energy is characteristic of the parent atom, and the technique can be used to determine relative amounts of elements.

$$E_A = (E1 - E3) - E3 = E1 - 2E3 \qquad 1\text{-}3$$

1.4 Organization of the thesis

The goal of this study was to explore the use of photochemical metal organic deposition (PMOD) to prepare metal oxide multilayer films. Two components chosen to fabricate multilayer films were titanium oxide and manganese oxide. These materials were chosen to investigate for the following reasons. First, they have widely different properties. Second, it has been found that titanium oxide film can be formed by photolysis of $Ti(acac)_2(i\text{-}prop)_2$ ($i\text{-}prop = OCH(CH_3)_2$; $acac = CH_3COCHCOCH_3$) and manganese oxide can be formed by photolysis of $Mn(O_2CCH(C_2H_5)C_4H_9)_2$.[9] Third, photochemical reaction time for each of these precursors is short. This should result in shorter time to fabricate multilayer samples.

But little information about photo-decomposition mechanism of the two precursors $Ti(acac)_2(i\text{-}prop)_2$ ($i\text{-}prop = OCH(CH_3)_2$; $acac = CH_3COCHCOCH_3$) and $Mn(O_2CCH(C_2H_5)C_4H_9)_2$ was known. Prior to the fabrication of the multilayer films, it was useful to investigate the mechanism of the photochemical reaction of $Ti(acac)_2(i\text{-}$

prop)$_2$ precursor film on the silicon chip and to study the properties of the photoproduced titanium oxide films. It was also necessary to investigate the mechanism of photochemical reaction of $Mn(O_2CCH(C_2H_5)C_4H_9)_2$ precursor film on the silicon chip and to study the properties of the manganese oxide films.

Chapter 2 gives the preparation and characterization of titanium oxide films produced from $Ti(acac)_2(i\text{-prop})_2$ films on a silicon chip. The use of Fourier Transform Infrared (FTIR) spectroscopy to monitor the photolysis of $Ti(acac)_2(i\text{-prop})_2$ will be presented. The volatile products from the photolysis of $Ti(acac)_2(i\text{-prop})_2$ were identified with mass spectrometry. The composition of the film produced by photolysis of $Ti(acac)_2(i\text{-prop})_2$ was determined by Auger electron spectroscopy. These experiments provided us with the information for the mechanistic study. The use of x-ray diffraction to further characterize the photoproduced film produced from $Ti(acac)_2(i\text{-prop})_2$ will also be presented in Chapter 2.

Chapter 3 deals with preparation and characterization of manganese oxide films produced from $Mn(O_2CCH(C_2H_5)C_4H_9)_2$ films on a silicon chip. The use of Fourier Transform Infrared (FTIR) spectroscopy to monitor the photolysis of $Mn(O_2CCH(C_2H_5)C_4H_9)_2$ will be presented. The volatile products from the photolysis of $Mn(O_2CCH(C_2H_5)C_4H_9)_2$ will be identified by mass spectroscopy. The results of Auger electron spectroscopy of the film produced by photolysis of $Mn(O_2CCH(C_2H_5)C_4H_9)_2$ will be presented. These results are reconciled in the form of a proposed mechanism. The use of x-ray diffraction to identify the phase of the photoproduced film of $Mn(O_2CCH(C_2H_5)C_4H_9)_2$ will also be presented in Chapter 3.

Following the study of the titanium compound and the manganese compound, we fabricated multilayer samples of alternating titanium and manganese oxides. Thermal treatment was performed on the multilayer sample. Low angle x-ray diffraction provided us with the information about the layered structure. High angle x-ray diffraction provided us with the information of phase identification. The detailed results are reported in Chapter 4.

Chapter 2 Preparation and characterization of titanium oxide films

2.1 Introduction

In this chapter, deposition of titanium dioxide by means of photochemical metal organic deposition (PMOD) will be described. Titanium dioxide films have attracted extensive attention during the last decade due to their optical and electric properties.[10] A variety of methods have been used to form titanium dioxide thin films; these include magnetron sputtering of TiO_2,[11-13] metalorganic chemical vapor deposition[10] and chemical vapor deposition.[14]

There are certain criteria for an ideal precursor. PMOD is based on a photochemical reaction, so the precursor has to be photosensitive. When dissolved in a volatile solvent, it must form an amorphous film upon spin coating on the substrate. The precursor must also be nonvolatile and thermally stable.

Considering the above criteria and the results obtained previously in our laboratory,[9] the titanium complex $Ti(acac)_2(i\text{-}prop)_2$ (i-prop = $CHO(CH_3)_2$; acac = $CH_3COCHCOCH_3$), shown in Figure 2-1, was chosen as a precursor.[16] It had been shown that photolysis of a $Ti(acac)_2(i\text{-}prop)_2$ film resulted in the loss of all IR absorption associated with the ligands and Auger analysis showed that TiO_2 film has been deposited on the substrate.

One goal of this study was to investigate the mechanism of the photochemical reaction of $Ti(acac)_2(i\text{-}prop)_2$ precursor film on the silicon chip. A second goal was to study the properties of the photoproduced titanium dioxide films. In order to reach these goals, the volatile photoproducts of $Ti(acac)_2(i\text{-}prop)_2$ precursor film were studied by

mass spectrometry. The films photogenerated from Ti(acac)$_2$(i-prop)$_2$ photolysis were studied by both Auger electron spectroscopy and X-ray powder diffraction. Finally, a mechanism for the photoreaction of Ti(acac)$_2$(i-prop)$_2$ complex as a thin film on silicon surfaces will be proposed. The study of the single component films described in this Chapter gave insight in the design of processing conditions to deposit multilayer films in Chapter 4.
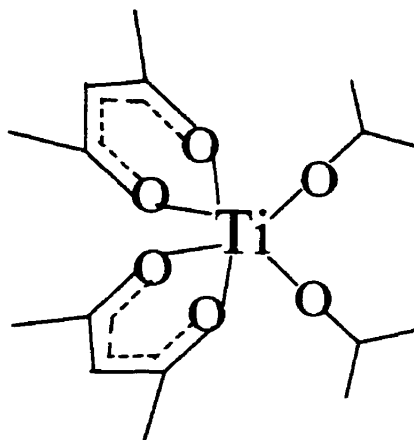
Figure 2-1   Structure of Titanium bis-acetylacetonate di-isopropoxide,

Ti(acac)$_2$(i-prop)$_2$

2.2 Results

2.2.1 Photolysis of Ti(acac)$_2$(i-prop)$_2$ films

A toluene isopropanol solution of Ti(acac)$_2$(i-prop)$_2$ was used as a precursor solution. The solution was spin coated to provide amorphous films of Ti(acac)$_2$(i-prop)$_2$ on a silicon chip. The films appeared to be uniform and featureless by optical inspection.

The FTIR spectrum of a film of Ti(acac)$_2$(i-prop)$_2$ was obtained by measuring the transmission through the sample. FTIR spectroscopic data of it are presented in Figure 2-2 and summarized in Table 2-1. Blair[9] has produced data similar to those in Table 2-1. Three absorption bands are assigned to the isopropoxide ligands: the absorption at 1012

cm^{-1} is assigned to $v_{as}(CO)$, the absorption at 991 cm^{-1} is assigned to $v_s(CO)$ and the absorption at 624 cm^{-1} is assigned to $v(TiO)$. The remaining absorption bands are assigned to the acac ligand. The band at 1607 cm^{-1} is assigned to $v(CC)$. The band at 1585 cm^{-1} is assigned to $v(CO)$. The band at 1523 cm^{-1} is assigned to $v(CO)$ coupled with $v(CC)$. The band at 1435 cm^{-1} is assigned to $v(CO)$ coupled with $\delta(CH)$. The band at 1381 cm^{-1} is assigned to $\delta_d(CH_3)$. The band at 1327 cm^{-1} is assigned to $\delta_s(CH_3)$. The band at 1276 cm^{-1} is assigned to $v(C-CH_3)$ coupled with $v(CC)$. The band at 1163 cm^{-1} is assigned to $\delta(CH)$ coupled with $v(C-CH_3)$. The band at 928 cm^{-1} is assigned to $v(CC)$ coupled with $v(CO)$. The band at 851 cm^{-1} is assigned to $\pi(CH)$. The band at 669 cm^{-1} is assigned to $\delta(C-CH_3)$ coupled with $v(TiO)$. The assignments were based on various metal acetylacetonate and metal alkoxide complexes[15-17].

The film of $Ti(acac)_2(i\text{-}prop)_2$ was irradiated with 254 nm light for 5 min. A second FTIR spectrum was obtained and is presented in Figure 2-2. A decrease in intensity of all the FTIR absorption bands associated with $Ti(acac)_2(i\text{-}prop)_2$ is observed. The experiment proceeded with alternating exposures to UV light and spectral analysis of FTIR. Figure 2-2 shows the FTIR spectra changes. A continuous decrease in intensity of all the FTIR absorption bands associated with $Ti(acac)_2(i\text{-}prop)_2$ is observed. The photolysis of $Ti(acac)_2(i\text{-}prop)_2$ for a total of 25 min resulted in the loss of all IR absorption bands associated with the acetylacetonate and iso-propoxide ligands. No new absorptions were observed. This indicates that there was no ligand containing intermediate formed.

Equation 2-1 is the photochemical reaction.

$$Ti(CH_3COCHCOCH_3)_2(CH_3CHOCH_3)_2 \xrightarrow{hv} TiO_x + \text{organic products} \qquad (2\text{-}1)$$
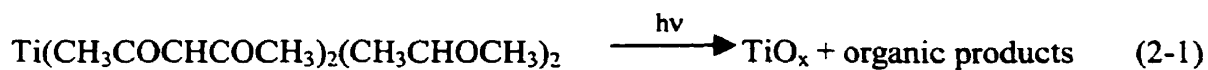
The lack of IR absorptions associated with the decomposition products of the ligands

forced us to turn to a different method to investigate the organic photoproducts.

Table 2-1 The FTIR spectroscopic data

of Ti(acac)$_2$(i-prop)$_2$ as a film on a silicon surface

Frequency (cm^{-1})	Band Assigment	ligand
1607	v(CC)	acac
1585	v(CO)	acac
1523	v(CO)+ v(CC)	acac
1435	v(CO)+ δ(CH)	acac
1381	δ$_d$(CH$_3$)	acac
1327	δs(CH$_3$)	acac
1276	v(C-CH$_3$)+ v(CC)	acac
1163	δ(CH)+v(C-CH$_3$)	acac
1012	v$_{as}$(CO)	i-prop
991	v$_s$(CO)	i-prop
928	v(CC)+ v(CO)	acac
851	π(CH)	acac
669	δ(C-CH$_3$)+ v(TiO)	acac
624	v(TiO)	i-prop

Figure 2-2 FTIR spectra of Ti(acac)$_2$(i-prop)$_2$ film

upon photolysis at 0, 5, 10, 15 and 25 minutes

2.2.2 Mass spectrometric analyses of volatile photoproducts formed by the photolysis of Ti(acac)$_2$(i-prop)$_2$ film

Mass spectrometric analysis of the volatile products formed from photolysis of a Ti(acac)$_2$(i-prop)$_2$ film on a silicon chip was conducted in order to determine the organic products. A Ti(acac)$_2$(i-prop)$_2$ film on a silicon chip was prepared by spin coating from

toluene isopropanol solution. The sample was irradiated with UV light in a vacuum chamber. The gas phase was then introduced into a Mass Spectrometer.

Table 2-2 below summaries the data and interpretation[18,19] of the MS of the volatile products from photolysis of Ti(acac)$_2$(i-prop)$_2$ film. The spectrum of MS had peaks at m/e of 100, 85, 84, 69, 58, 43 and 41. The peaks at m/e of 100, 85 and 43 are associated with acetylacetone (CH$_3$COCH$_2$COCH$_3$, m/e=100) and its fragments, COCH$_2$COCH$_3$ (m/e=85) and COCH$_3$ (m/e=43). The peaks at m/e of 84, 69, 43 and 41 corresponded to 3-pentene-2-one (CH$_3$COCH=CHCH$_3$, m/e=84) and its fragments, COCH=CHCH$_3$ (m/e=69), CH$_3$CO (m/e=43) and CH=CHCH$_3$ (m/e=41). The peaks at m/e of 58 and 43 corresponded to 2-propanone (CH$_3$COCH$_3$, m/e=58) and its fragment, COCH$_3$ (m/e=43).

Table 2-2 MS result of gas phase products from the photolysis of a film of Ti(acac)$_2$(i-prop)$_2$

m/e	assignment
100, 85, 43	acetylacetone (MeCOCH$_2$COMe)
84, 69, 43, 41	3-pentene-2-one (MeCOCH=CHMe)
58, 43	2-propanone (MeCOMe)

From the MS analysis result, the photochemical reaction is shown as equation 2-2.

$$\text{Ti(CH}_3\text{COCHCOCH}_3\text{)}_2\text{(CH}_3\text{CHOCH}_3\text{)}_2 \xrightarrow{hv} \text{TiO} + \text{CH}_3\text{COCH=CHCH}_3$$

$$+ \text{CH}_3\text{COCH}_2\text{COCH}_3 + 2\text{ CH}_3\text{COCH}_3 \qquad (2\text{-}2)$$
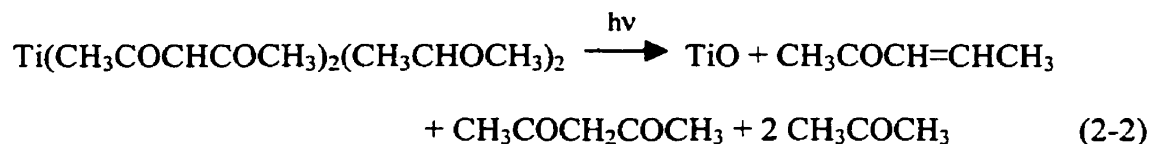
2.2.3 Auger electron analyses of films produced by the photolysis of Ti(acac)$_2$(i-prop)$_2$ films

In order to determine the elemental composition of the remaining film after Ti(acac)$_2$(i-prop)$_2$ photolysis, Auger electron analyses were carried out. A Ti(acac)$_2$(i-prop)$_2$ film on a silicon chip was prepared by spin coating from toluene isopropanol solution. It was irradiated until no bands from the ligands were observed in the FTIR spectrum. This indicated that all the ligands had been ejected from the film. The surface was cleaned by Argon ion sputtering for 15 sec. An Auger electron spectrum was then obtained.

The Auger electron spectrum of the sample prepared above is shown in Figure 2-3. The spectrum has peaks at 380, 418 and 502 eV. Peaks at 380, 418 eV are associated with titanium (LMM) and the peak at 502 eV is indicative of oxygen (KLL).[20] No other peaks were observed in the spectrum. This result indicates that the only elements existing on the film are Ti and O. Further argon ion sputtering for 15 sec followed by another Auger spectrum confirmed the peaks position and intensity. The second spectrum has the same appearance as the first one.

Table 2-3 lists the sputter time, peak intensity (peak-to-peak Auger amplitude), sensitivity factor and concentration of titanium and oxygen. It also includes the composition of the film obtained from the experiment. The calculated compositions were based upon the intensity of the oxygen signal at 502 eV and the titanium signal at 418 eV. The calculated composition of the film from two spectra was TiO$_{3\pm1}$. This elemental composition was approximate due to the 30% error of the AES from sensitivity factor. The film probably consisted of TiO$_2$, as Ti(IV) is the most stable oxidation state of

titanium.[21] The reported results of Blair[9] are within experimental error of those determined here.

From the balanced equation 2-2, it was found that photoreaction of Ti(acac)$_2$(i-prop)$_2$ film resulted in TiO film on the silicon chip. TiO film reacted with O$_2$ in the air generated TiO$_2$ film (equation 2-3).

$$TiO + \frac{1}{2} O_2 \text{ (in air)} \longrightarrow TiO_2 \qquad (2\text{-}3)$$

Table 2-3 Auger analysis of resultant film from Ti(acac)$_2$(i-prop)$_2$ photolysis

Sputter time (sec)	Relative intensity Ti	O	Sensitivity factor Ti	O	Concentration Ti	O (%)	Composition (calculated)
15	19.5±5	70.4±5	0.45	0.51	23±6	77±5	Ti$_6$O$_{19}$
30	20±6	69±6	0.45	0.51	25±7	75±6	TiO$_3$
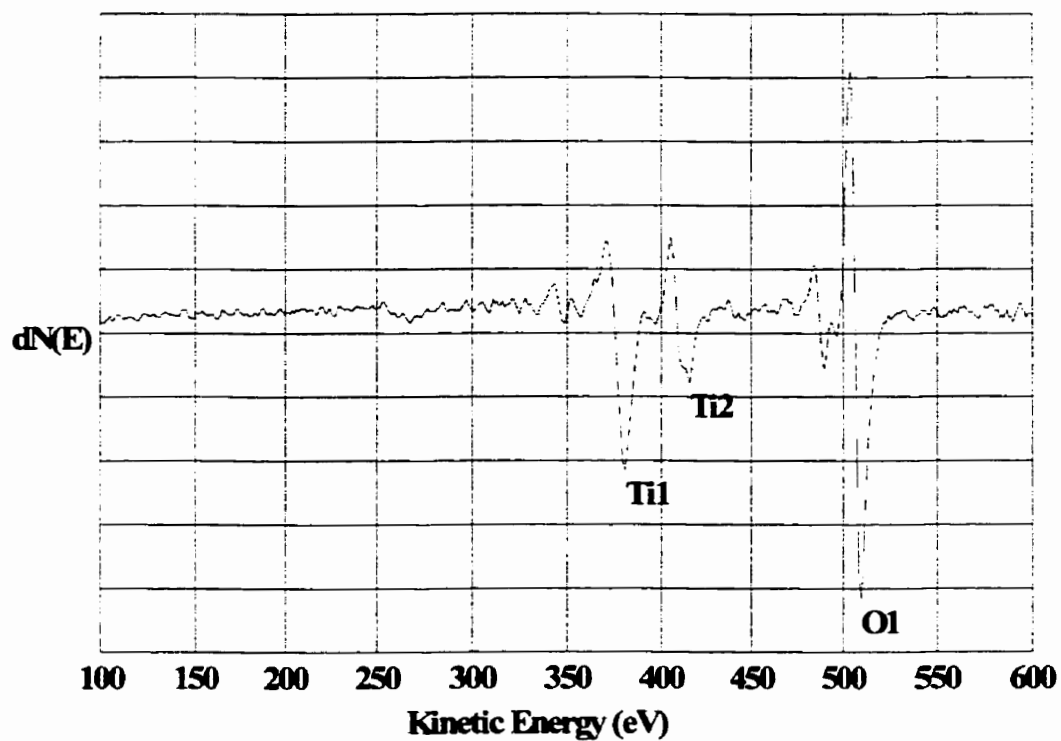
Figure 2-3 Auger electron spectrum of resultant film from Ti(acac)$_2$(i-prop)$_2$ photolysis

(following 15 sec of sputtering with argon ions energy to clean the film surface)

2.2.4 X-ray diffractions from films produced by the photolysis of Ti(acac)$_2$(i-prop)$_2$

From the Auger results (see section 2.2.3), it was found that the photolysis of the Ti(acac)$_2$(i-prop)$_2$ precursor film produced a TiO$_2$ film on the silicon chip. This film was further studied with X-ray powder diffraction. Figure 2-4 shows the diffraction spectrum of the film. The peak at 33° was from the n-Si(100) substrate. No peak from the film was observed. This clearly indicated that the film was amorphous. Equation 2-3 can be written as following:

$$TiO + \frac{1}{2} O_2 \text{ (in air)} \longrightarrow TiO_2 \text{ (amorphous)} \qquad (2\text{-}4)$$
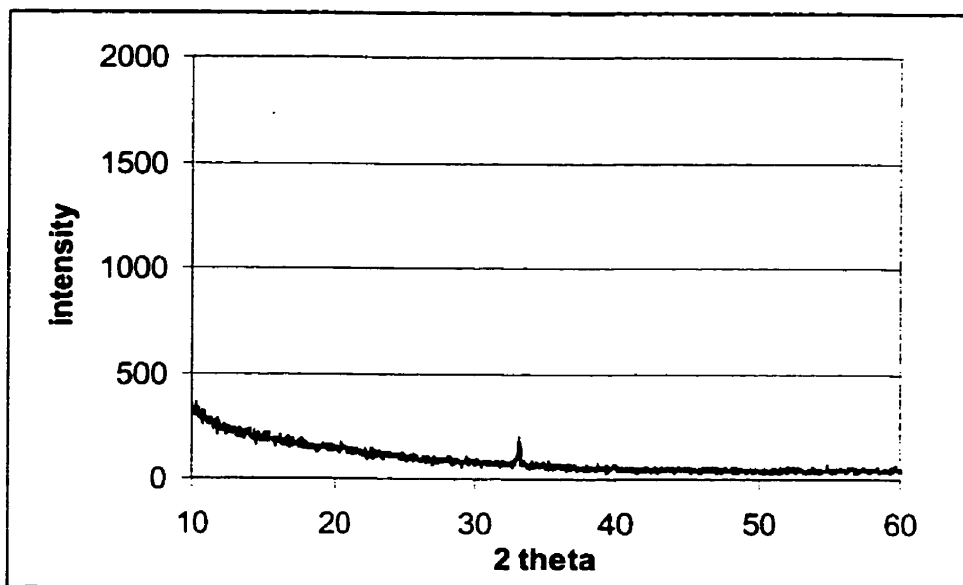
Figure 2-4 X-ray powder diffraction spectrum of the film photoproduced from
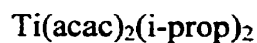
Ti(acac)$_2$(i-prop)$_2$

In order to study the crystallization of the TiO_2 amorphous films, XRD spectra were obtained on a series of heated films. A $Ti(acac)_2(i\text{-prop})_2$ film on a silicon chip was prepared by spin coating from a toluene isopropanol solution. It was irradiated until no bands from the ligands were observed in FTIR. The film on silicon chip then was heated at 300 °C for 2 hr. Figure 2-5 a) shows the XRD spectrum collected of the film after heating. The peak at 33° was from the n-Si(100) substrate. No peaks from the film were observed. This clearly indicated that the film still was amorphous after 300 °C heating.

In a similar experiment, another film was prepared. It was heated at 500 °C for 2 hr. Figure 2-5 b) shows the XRD spectrum collected of the film. The peaks at $2\theta = 25°$, 38 °, 48 °, 54 ° and 55 °were observed. They corresponded to the reflections from the anatase (101), (004), (200), (105) and (211) planes.[22] These data indicated that amorphous film crystallized to yield polycrystalline anatase on the silicon chip upon thermal treatment.

Repeating the experiment but heating at 700 °C instead of 500 °C resulted in the same product. Polycrystalline anatase was formed on the silicon chip.

In a similar experiment, a film was heated at 900 °C for 2 hr. Figure 2-5 d) shows the XRD spectrum collected of the film. It shows the peaks at 25 °, 38 °, 48 °, 54 ° and 55 °. They corresponded to the same anatase planes as those in Figure 2-5 c). The X-ray diffraction spectrum also shows peaks at 27 °, 36 °, 39 °, 41 °, 44 °, 54 ° and 57 °. These corresponded to reflections from the (110), (101), (200), (111), (210), (211) and (220) planes of rutile.[23] This indicated that the film was composed of a mixture of anatase and rutile.

A film prepared the same way as above was heated at 1100 °C for 2 hr. Figure 2-5 e) shows the XRD spectrum. It shows the peaks at 2θ =27°, 36°, 39°, 41°, 44°, 54° and 57°. They correspond to the rutile reflections of the (110), (101), (200), (111), (210), (211) and (220) planes. This film was composed of polycrystalline rutile.
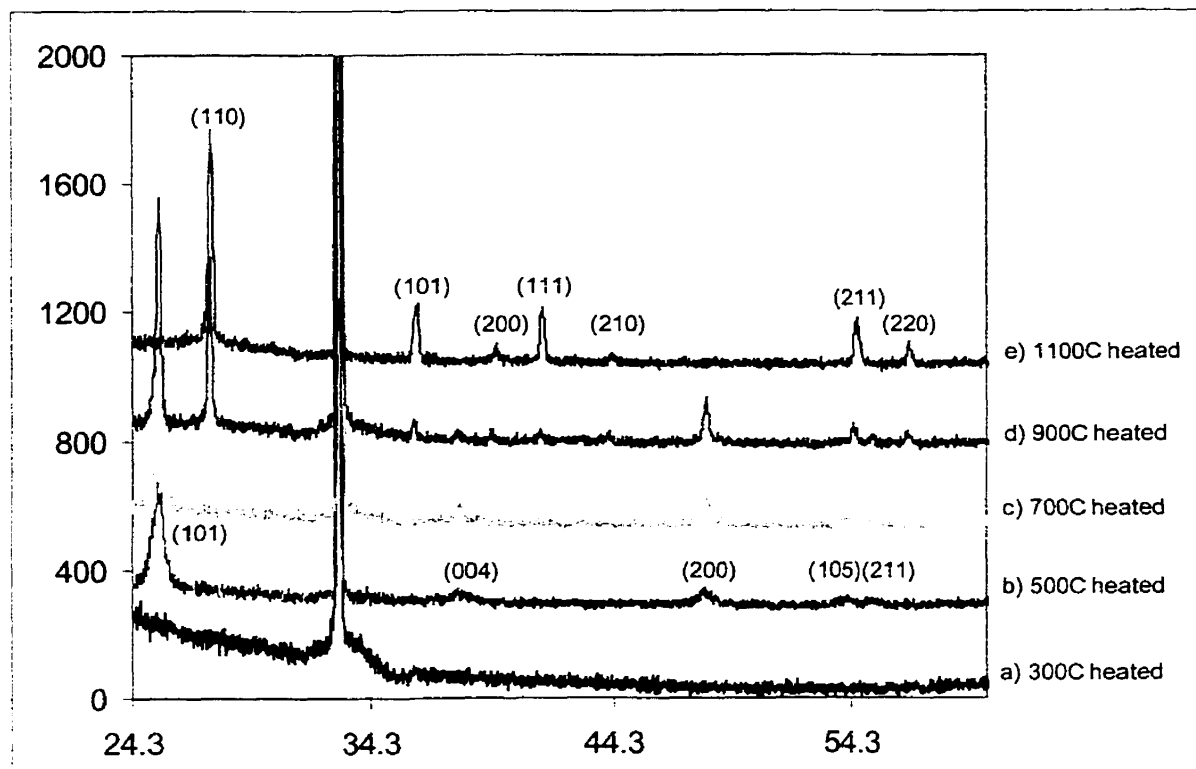
Figure 2-5 X-ray powder diffraction spectra collected on titanium dioxide film after heated for 2 hr at 300°C, 500 °C, 700 °C, 900 °C and 1100 °C

The thermal reactions of TiO_2 films on the silicon chip are shown in equations 2-5, 2-6 and 2-7.

$$TiO_2 \text{ (amorphous)} \xrightarrow{500^{\circ}C-700^{\circ}C} TiO_2 \text{ (anatase)} \qquad (2\text{-}5)$$

$$TiO_2 \text{ (amorphous)} \xrightarrow{700^{\circ}C-1100^{\circ}C} TiO_2 \text{ (mixture of anatase and rutile)} \qquad (2\text{-}6)$$

$$TiO_2 \text{ (amorphous)} \xrightarrow{1100^{\circ}C} TiO_2 \text{ (rutile)} \qquad (2\text{-}7)$$
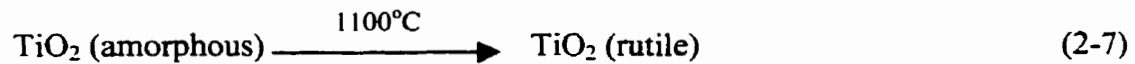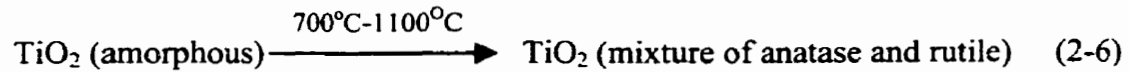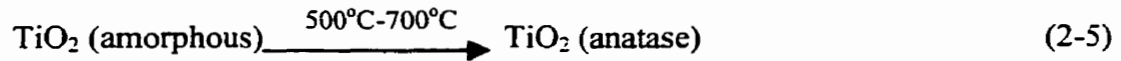
The unit cells of rutile and anatase are tetragonal. In both rutile and anatase structure, Ti^{4+} ion is surrounded by an irregular octahedra of oxide ions. The number of edges shared by the octahedra is two out of twelve in rutile. The number of edges shared by the octahedra is four out of twelve in anatase.[24]

2.3 Discussion

It has been shown that the Ti(acac)$_2$(i-prop)$_2$ precursor solution could form a uniform film through spin coating. FTIR spectroscopy indicated that all the ligands of Ti(acac)$_2$(i-prop)$_2$ have been ejected from the film upon irradiation under UV light. From MS, it was found that the volatile products upon irradiation were acacH, 3-pentene-2-one and 2-propanone. Auger electron spectroscopy indicated that the photolysis of Ti(acac)$_2$(i-prop)$_2$ generated TiO$_2$ as the film remaining on the silicon chip. X-ray powder diffraction indicated that the film remaining on the silicon chip was amorphous. The reactions of Ti(acac)$_2$(i-prop)$_2$ film, shown in equations 2-8 and 2-9, summarize all these results.

$$Ti(CH_3COCHCOCH_3)_2(CH_3CHOCH_3)_2 \xrightarrow{h\nu} TiO + CH_3COCH=CHCH_3$$
$$+ CH_3COCH_2COCH_3 + 2\ CH_3COCH_3 \quad (2\text{-}8)$$

$$2\ TiO + O_2\ (\text{in air}) \longrightarrow 2\ TiO_2\ (\text{amorphous}) \quad (2\text{-}9)$$
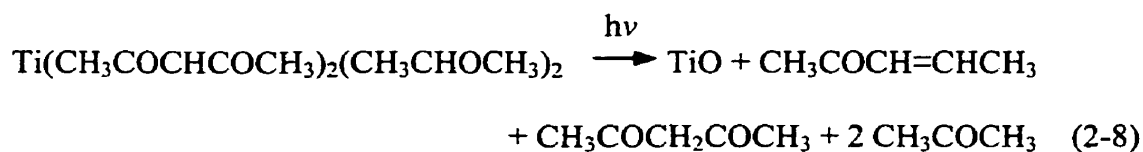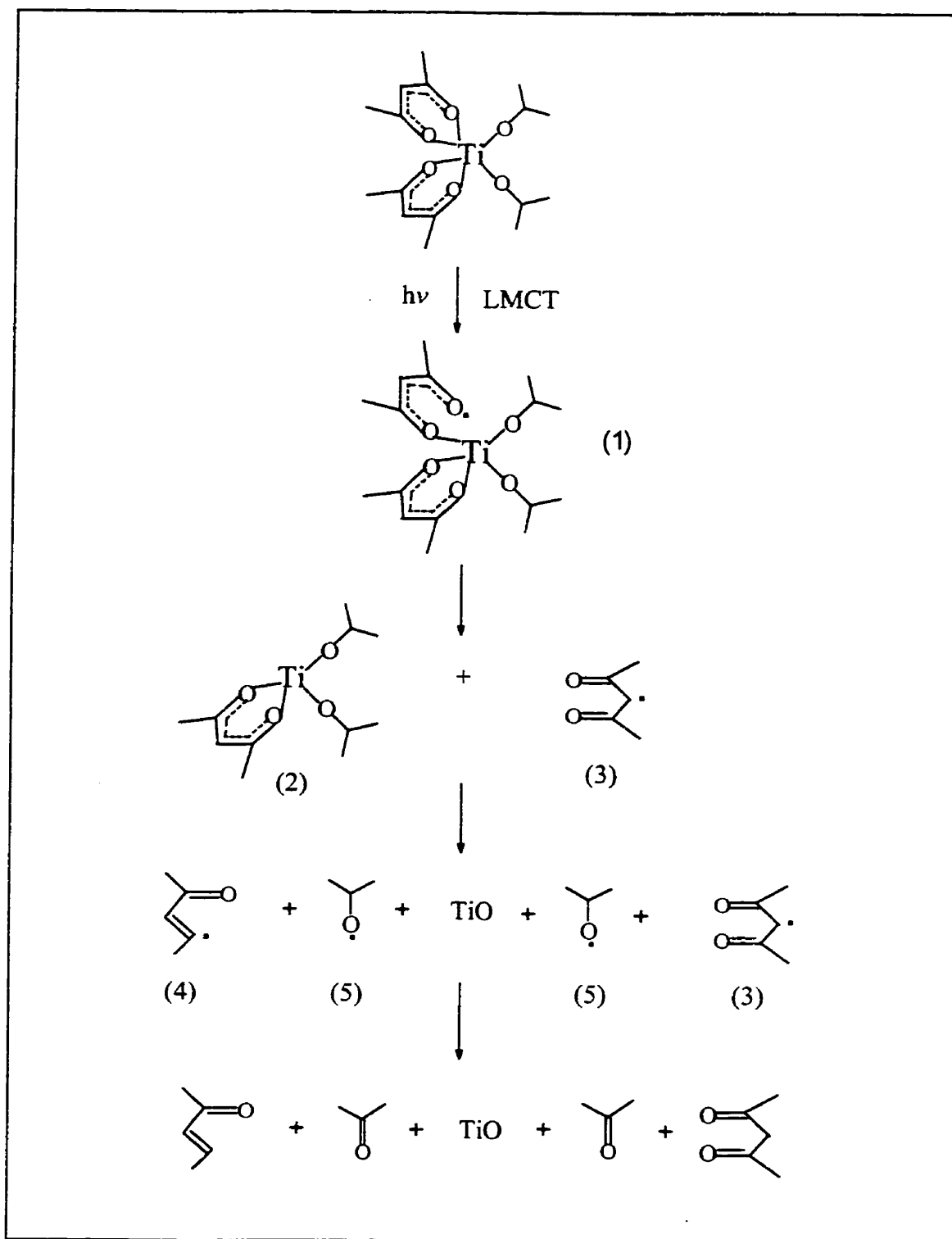
Figure 2-6 Mechanism for the photo-decomposition of Ti(acac)$_2$(i-prop)$_2$

27

The proposed mechanism for the photo-decomposition of Ti(acac)$_2$(i-prop)$_2$ forming TiO (equation 2-8), shown in Figure 2-6, is consistent with all these results.[25]

The reaction is initiated by the absorption of a photon which result in ligand-to-metal charge transfer transition in the starting material, Ti(acac)$_2$(i-prop)$_2$. The transition results in cleaving a titanium oxygen bond of acac ligand. The diradical species (1) is formed. The complex (1) contains both organic centered radical and titanium in the (III) oxidation state. As a result we expect (1) to be very reactive. The unstable species (1) fragments to form (2) and (3). (2) is unstable as it consists of the highly reactive Ti (III). It undergoes fragmentation to form a radical species (4), two radical species (5) and TiO. This fragmentation presumably occurs in a multistage process. The hydrogens transfer from species (5) to species (3) and (4) lead to 2- propanone, 3-pentene-2-one and acacH. All of these organic products were observed in the MS spectrum.

The photoreaction of Ti(acac)$_2$(i-prop)$_2$ film resulted in TiO film on the silicon chip. The photoproduced TiO reacting with O$_2$ in air generated the TiO$_2$ film. X-ray powder diffraction indicated that the TiO$_2$ film on the silicon chip was amorphous.

Heating the amorphous film resulted in its crystallization. Crystallization temperature has a strong influence on the structure of the films. At crystallization temperatures of 500°C and 700, polycrystalline anatase was formed. At intermediate temperatures between 700 and 1100 °C both anatase and rutile were found. Heating in air up to 1100 °C, polycrystalline rutile formed.

Martin et al.[13] have studied the heating temperature of TiO$_2$ films deposited by reactive r.f. magnetron sputtering. They have obtained results consistent with ours. In their study anatase was transformed to rutile between 700 and 900 °C. It has been

28

reported that the rutile form of TiO_2 is its most stable form.[24] Both anatase and brookite

transform to rutile irreversibly on heating. The transformation temperature depends on

the method of preparation of the sample[13]. Therefore, our experiment results were

consistent with all those reported.

2.4 Conclusion

The photochemical deposition of titanium dioxide films through thin films of

$Ti(acac)_2(i-prop)_2$ precursor has been demonstrated. The photochemistry of $Ti(acac)_2(i-prop)_2$ has been studied by FTIR, MS and Auger electron spectroscopy.

The $Ti(acac)_2(i-prop)_2$ precursor film absorbs photons upon UV irradiation

undergoing a ligand-to-metal charge transfer transition. This transition finally leads to

generate TiO, acacH, 2-propanone and 3-pentene-2-one.

The photoproduced TiO film reacts with O_2 in air resulting in amorphous films of

TiO_2 on silicon substrate.

Anatase and rutile were successfully formed upon thermal heating. A mixture of both

anatase and rutile phases has been observed between 700 and 1100 °C.

2.5 Experimental section

2.5.1 Instruments and materials

N-type Si(100) wafers obtained from Shin Etsu were used in these studies. The

silicon was cut to the approximate dimensions 10×14mm as needed. It was cleaned by

acetone before using. An in house built spin coater was used to coat films on the silicon

chip.

The Ti(acac)$_2$(i-prop)$_2$ precursor was obtained commercially from Aldrich Co. It was obtained as a 75 % solution in isopropanol.

The photolysis of the Ti(acac)$_2$(i-prop)$_2$ film was monitored by FTIR spectroscopy. The photolysis beam was from a UVP Inc. model UVG-54 short wave UV-254nm lamp except in section 2.5.3. The photolysis beam in section 2.5.3 was from an Oriel spectral calibration UV lamp. The FTIR spectra were obtained with 4 cm^{-1} resolution using a Bomem MB-120 FTIR spectrophotometer.

The mass spectra were recorded with a HP 5958 gas chromatography-MS spectrometer. An electron-impact ion source was used and the ion source temperature was 200 °C. The resolution was 1000 amu^{-1}. The electron energy for ionization was 70 eV. The scanning mass range was 5-120 m/z.

Auger spectra were obtained using a PHI double pass CMA at 0.85 eV resolution at the Surface Analysis Laboratory, Department of Physics, Simon Fraser University.

XRD spectra were obtained using an X-ray generator system (Model: PW1730 Philips Electronic Instruments Inc.) with Cu K$_\alpha$ radiation, Department of Physics, Simon Fraser University.

2.5.2 Preparation and photolysis of Ti(acac)$_2$(i-prop)$_2$ films

An FTIR spectrum of a silicon chip was obtained prior to the film deposition and used as a reference. The silicon chip was placed on the platform of a spinner. It was secured on the platform with double-sided tape. 0.1230g of Ti(acac)$_2$(i-prop)$_2$ complex solution was mixed with 1.2401g of toluene. A few drops of this solution were dispensed from a disposable pipette onto the stationary silicon chip, then spun at 2800 rpm. The

chip was spun until the solvent had evaporated (approximately 1 min) and a thin film of precursor remained on the chip.

An FTIR spectrum of the precursor film was obtained. The sample was irradiated with 254 nm light for 5 min. Another FTIR spectrum was obtained. This procedure was repeated for accumulated photolysis times of 10, 15 and 25 min at which the FTIR bands due to the ligands in the $Ti(acac)_2(i-prop)_2$ no longer were observed (see Figure 2-2).

2.5.3 Mass spectrometric analysis of volatile products produced in the photolysis of $Ti(acac)_2(i-prop)_2$ films

The volatile photoproducts from a film of $Ti(acac)_2(i-prop)_2$ on a silicon chip were analyzed with a Mass spectrometer. The chamber shown in Figure 2-7 was used to collect volatile products from photolysis of films. The chamber is made of quarz in order to let the photolysis beam pass through it. An Oriel spectral calibration UV lamp was used to irradiate the precursor films in the chamber.

A sample of the $Ti(acac)_2(i-prop)_2$ complex 75% in isopropanol 0.08 g (obtained from Aldrich Co.) was mixed with 0.45g of toluene. A drop of this solution was dispensed from a disposable pipette onto the stationary silicon chip, then spun at 2200 rpm. The chip was spun until the solvent had evaporated (approximately 1 min) and a thin film of precursor remained on the chip.
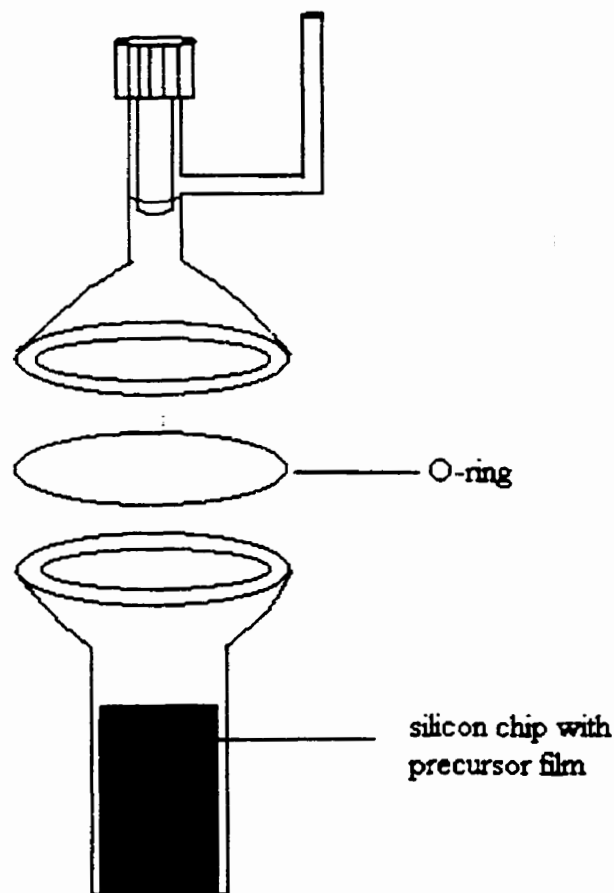
Figure 2-7 A chamber used for collecting MS sample

The sample was placed in the bottom part of a glass chamber. Then, the top and the bottom parts of the device were joined with a greased o-ring. After evacuation of the chamber by a vacuum pump for an hour, the valve was closed. The sample in the sealed chamber was then irradiated for 25 min with UV lamp.

The chamber with the sample was connected to a mass spectrometer. The mass spectrum of background was recorded and then the spectrum of the sample was recorded. The spectra of the volatile products were obtained by subtracting that of background from the sample spectra. The MS results are summarized in Table 2-2.

2.5.4 Auger analysis of photoproduced film from Ti(acac)$_2$(i-prop)$_2$

A Ti(acac)$_2$(i-prop)$_2$ precursor film was prepared exactly the same as that described in section 2.5.3. The film was then irradiated under the UV light for 4 hr. An FTIR spectrum of the film was obtained conforming that no bands associated with precursor ligands were evident. The sample was then moved to Auger electron spectrometer for analysis. The results are summarized in Table 2-3.

2.5.5 Thermal treatment of films produced from Ti(acac)$_2$(i-prop)$_2$

A Ti(acac)$_2$(i-prop)$_2$ precursor film was prepared as described in section 2.5.3. The film was irradiated under the UV light for 4 hr. The photoproduced film on silicon chip was heated at 300 °C in an oven for 2 hr. An XRD spectrum was obtained after heating. The preparation of the other samples was similar to the one described above. The amorphous films were obtained from the photolysis of Ti(acac)$_2$(i-prop)$_2$ precursor films. The films were heated at temperatures of 500 °C, 700 °C, 900 °C and 1100 °C respectively in an oven for 2hr. The XRD spectrum was obtained following the heat treatment. The results are shown in Figure 2-5.

Chapter 3 Preparation and characterization of

manganese oxide films

3.1 Introduction

In this chapter, the photochemistry of amorphous films of $Mn(O_2CCH(C_2H_5)C_4H_9)_2$ to form manganese oxide will be presented. Manganese oxide films are technologically important materials with a variety of applications, such as electrode materials for lithium secondary batteries[26] and corrosion inhibiting agents for paints.[27] Different methods have been used to produce manganese oxide films, e.g. reactive evaporation,[26] sol-gel and electrodeposition.[28]

The main objective of this study was to investigate the detail of the photochemical reaction of a $Mn(O_2CCH(C_2H_5)C_4H_9)_2$ film on a silicon chip. This complex was selected because it could form an amorphous film upon spin coating on a substrate and it is photosensitive. It had been shown by Blair in our laboratory[9] that photolysis of a $Mn(O_2CCH(C_2H_5)C_4H_9)_2$ film resulted in the loss of all IR absorption associated with the ligands while Auger electron spectroscopy indicated that a manganese oxide film had been produced on the silicon chip.

In this study, one goal was to investigate the mechanism of the photochemical reaction of a $Mn(O_2CCH(C_2H_5)C_4H_9)_2$ precursor film on a silicon chip. A second goal was to study the properties of the photoproduced manganese oxide films. In order to reach these goals, the volatile photoproducts of $Mn(O_2CCH(C_2H_5)C_4H_9)_2$ precursor film were studied by mass spectrometry. The photoproduced films were studied by both Auger electron spectroscopy and X-ray powder diffraction. The study of the single

component films in this Chapter helped us in the design of processing conditions to deposit the multilayer films described in Chapter 4.

3.2 Results

3.2.1 Characterization of $Mn(O_2CCH(C_2H_5)C_4H_9)_2$ film

A mineral spirits hexane solution of $Mn(O_2CCH(C_2H_5)C_4H_9)_2$ was used as the precursor solution. The solution was spin coated to provide an amorphous film on a silicon chip. The film appeared to be uniform and featureless by optical inspection.

The FTIR spectrum of a $Mn(O_2CCH(C_2H_5)C_4H_9)_2$ film was obtained by measuring the transmission through the sample. The FTIR spectrum is shown in Figures 3-1 and 3-2.

Figure 3-1 shows the FTIR spectrum of the $Mn(O_2CCH(C_2H_5)C_4H_9)_2$ film at the range from 2500 to 3300 cm^{-1}. All of the bands observed in this region are associated with the hydrocarbon chain of the ligand.[15] The absorption band at 2961 cm^{-1} is assigned to $v_{as}(CH_3)$. The absorption band at 2937 cm^{-1} is assigned to $v_{as}(CH_2)$. The absorption band at 2876 cm^{-1} is assigned to $v_s(CH_3)$. The absorption band at 2853 cm^{-1} is assigned to $v_s(CH_2)$. The assignment of FTIR bands in this region is summarized in Table 3-1.

Figure 3-2 shows the FTIR spectrum of the $Mn(O_2CCH(C_2H_5)C_4H_9)_2$ film at the range from 1200 to 1800 cm^{-1}. The bands in this region are associated with the carboxylate group of the ligand. The absorption band at 1693 cm^{-1} is assigned to the antisymmetric CO_2 stretch in the compound. It is from the coordinated 2-ethylhexanoate acid in the precursor.[29] The absorption band at 1589 cm^{-1} is assigned to $v_{as}(CO_2)$ of the 2-

ethylhexanoate ligands. Two absorption bands at 1464 and 1411 cm^{-1} are observed as a result of the coupling of the $\nu_s(CO_2)$ on different 2-ethylhexanoate ligands.[29,30] The assignment of the FTIR bands in this region is summarized in Table 3-1.
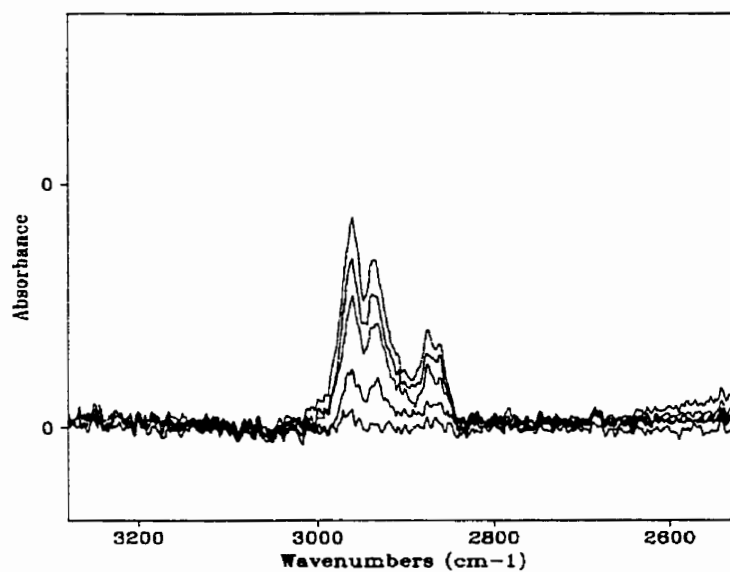
Figure 3-1 FTIR spectra of a $Mn(O_2CCH(C_2H_5)C_4H_9)_2$ film

upon photolysis for 0, 5, 10, 25 and 45 minutes (2500-3300 cm^{-1})
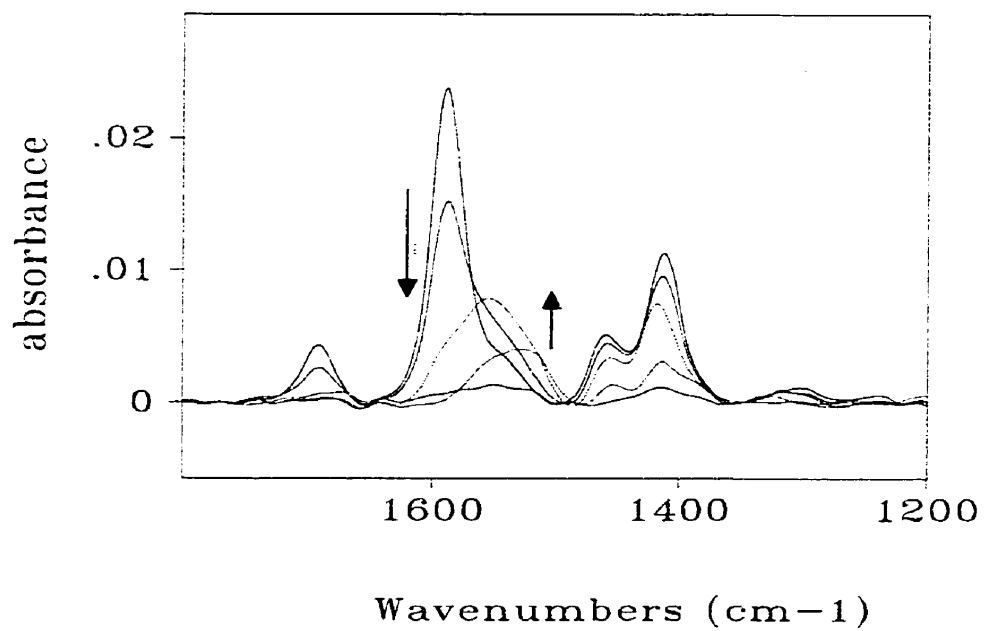
Figure 3-2 FTIR spectra of a $Mn(O_2CCH(C_2H_5)C_4H_9)_2$ film

upon photolysis for 0, 5, 10, 25 and 45 minutes (1200-1800 cm^{-1})

Table 3-1 The FTIR absorption band assignment for $Mn(O_2CCH(C_2H_5)C_4H_9)_2$

Frequency (cm^{-1})	Band Assignment	ligand
2961	$\nu_{as}(CH_3)$	2-ethylhexanoate
2937	$\nu_{as}(CH_2)$	2-ethylhexanoate
2876	$\nu_s(CH_3)$	2-ethylhexanoate
2853	$\nu_s(CH_2)$	2-ethylhexanoate
1693	$\nu_{as}(CO_2)$	2-ethylhexanoic acid
1589	$\nu_{as}(CO_2)$	2-ethylhexanoate
1464	$\nu_s(CO_2)$	2-ethylhexanoate
1411	$\nu_s(CO_2)$	2-ethylhexanoate

The frequency difference between the antisymmetric and symmetric stretches [$\Delta\nu = \nu_{as}(CO_2) - \nu_s(CO_2)$] has been used to distinguish the types of bonding of carboxylates with metals. The $\Delta\nu$ value decreases in the order unidentate > ionic > bridging > bidentate.[15]

From the FTIR results, it was found that $\Delta\nu = 125$ cm^{-1} for the $Mn(O_2CCH(C_2H_5)C_4H_9)_2$ film. The $\Delta\nu$ value is close to the expected value for a bridging carboxylate group. Figure 3-3 shows the bonding mode of carboxylate ligand with manganese, which was indicated by the FTIR spectrum.
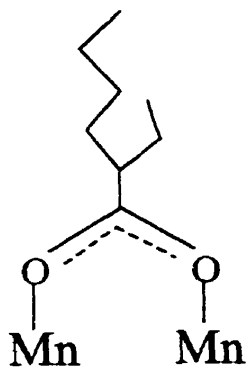
Figure 3-3 Bonding mode of carboxylate ligand with manganese in

$Mn(O_2CCH(C_2H_5)C_4H_9)_2$ film
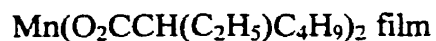
There is an absorption band at 1693 cm^{-1} associated with $v_{as}(CO_2)$ of the coordinated

2-ethylhexanoate acid in the precursor. Figure 3-4 shows the expected bonding of the

coordinated 2-ethylhexanoic acid in the precursor film.
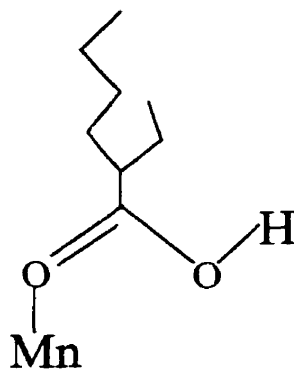
Figure 3-4 Coordinated 2-ethylhexanoic acid

The information from FTIR is not sufficient to find out the molecular structure of $Mn(O_2CCH(C_2H_5)C_4H_9)_2$. It could be a complex structure, which contains chains or clusters with the bonding modes shown in Figures 3-3 and 3-4. Further consideration of the nature of the precursor film is deferred to the discussion 3.3.

3.2.2 Photolysis of $Mn(O_2CCH(C_2H_5)C_4H_9)_2$ film

The film of $Mn(O_2CCH(C_2H_5)C_4H_9)_2$ was irradiated with a 254 nm light. The spectral changes associated with photolysis are presented in Figures 3-1 and 3-2. The photolysis for 5 minutes resulted in a loss of FTIR absorption bands intensity associated with the precursor. The absorption bands associated with both the hydrocarbon moiety at 2961, 2937, 2876 and 2853 cm^{-1} and the carboxylate group at 1589, 1464 and 1411 cm^{-1} all decreased in intensity. The absorption band associated with 2-ethylhexanoic acid at 1693 cm^{-1} also decreased in intensity. In addition to these changes, the appearance of a single broad absorption band at 1550 cm^{-1} was observed.

The loss of absorption bands associated with the precursor is indication of its photoreaction. The new absorption band at 1550 cm^{-1} is presumably associated with a photoproduct of the precursor.

Upon photolysis for 10 min, the broad band at 1550 cm^{-1} increased to maximum. The absorption at 1693 cm^{-1} due to the coordinated 2-ethylhexanoic acid was lost. The absorption bands associated with $v_s(CO_2)$ at 1464 and 1411 cm^{-1} and $v_{as}(CO_2)$ at 1589 cm^{-1} decreased in intensity (Figure 3-2). The absorption band at 1589 cm^{-1} is no longer apparent at this point in the photolysis. The overlap of the 1589 cm^{-1} band due to the

40

precursor and the 1550 cm^{-1} band of the intermediate lead to a large uncertainty of the amount of the 1589 cm^{-1} band remaining. The absorption bands at 1464 and 1411 cm^{-1} approached an absorbance of roughly 60% of the original absorbance. It is also observed from Figure 3-1 that following photolysis for 10 min, the absorption bands from C-H vibrations at 2961, 2937, 2876 and 2853 cm^{-1} approached an absorbance of roughly 60% of the original absorbance.

The loss of 40 % of the intensity associated with the C-H vibrations is indication of the loss of 40 % of the ligand from the film. This is based on the assumption that the transition probability for these bands is unlikely to be significantly changed upon reaction. Unexpectedly the $v_s(CO_2)$ show a similar decrease even though it would not be unexpected to see a change in extinction coefficient as a result of a chemical change. Based on these conclusions and the loss of the absorption band at 1589 cm^{-1}, we can now assign the absorption bands associated with the intermediate. The absorption bands at 1550, 1464 and 1411 cm^{-1} are all associated with the intermediate. Additionally, the absorption bands at 2961, 2937, 2876 and 2853 cm^{-1} are also associated with the intermediate. The absorption bands at 1464 and 1411 cm^{-1} are assigned as due to $v_s(CO_2)$. The absorption band at 1550 cm^{-1} is associated with $v_{as}(CO_2)$. The absorption band at 2961 cm^{-1} is assigned to $v_{as}(CH_3)$. The absorption band at 2937 cm^{-1} is assigned to $v_{as}(CH_2)$. The absorption band at 2876 cm^{-1} is assigned to $v_s(CH_3)$. The absorption band at 2853 cm^{-1} is assigned to $v_s(CH_2)$.

The frequency difference between the antisymmetric and symmetric stretches [$\Delta v = v_{as}(CO_2) - v_s(CO_2)$] is 86 cm^{-1} for intermediate film. The Δv value is close to the expected value for a bidentate carboxylate group. The FTIR of the intermediate is

41

consistent with the bonding mode shown in Figure 3-5. The information from FTIR is

not sufficient to predict the molecular structure of the intermediate. For convenience, we

will assign the formula of the intermediate film as $Mn(O_2CCH(C_2H_5)C_4H_9)_x$.
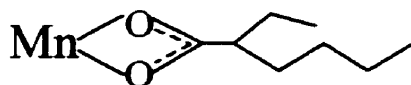
Figure 3-5 Bonding mode of carboxylate ligand with manganese in intermediate

The photochemical reaction from starting precursor to the formation of the

intermediate is proposed in equation 3-1.

$$2\ Mn(O_2CCH(C_2H_5)C_4H_9)_2 \xrightarrow{h\nu} Mn(O_2CCH(C_2H_5)C_4H_9)_x$$

$$+\ Mn + organic\ products \qquad (3\text{-}1)$$
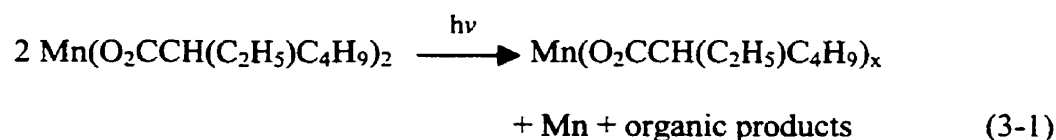
The intermediate film was further irradiated with 254 nm light for another 15 min.

Upon photolysis, the absorption bands at 2961, 2937, 2876 and 2853 cm^{-1}, which is

associated with C-H bonds, decreased. The absorption bands at 1464 and 1411 cm^{-1},

which is associated with $v_s(CO_2)$, also decreased. The absorption band at 1550 cm^{-1},

which is associated with $v_{as}(CO_2)$, not only decreased but also shifted to lower

wavenumber.

The loss of these absorption bands in intensity is indication of the loss of ligands from the intermediate. The absorption band shift around 1550 cm^{-1} is presumably due to a large and changing range of specific compounds in the film during photolysis process.

Upon a further 20 minutes photolysis, all the absorption bands associated with the intermediate were lost. This indicated the loss of all the ligands.

The photochemical reaction from the intermediate to final product is proposed in equation 3-2. The FTIR did not indicate the identity of the organic products of the reaction. We next turned to mass spectrometry to identify these products.

$$Mn(O_2CCH(C_2H_5)C_4H_9)_x \xrightarrow{\quad h\nu \quad} Mn + organic\ products \qquad (3-2)$$

3.2.3 Mass spectrometric analyses of the volatile products formed by the photolysis of Mn(O$_2$CCH(C$_2$H$_5$)C$_4$H$_9$)$_2$ films

As we mentioned above, mass spectrometry was used for the identification of the volatile organic photoproducts. In the initial stages of the photochemical reaction, the FTIR result indicated that a metal containing intermediate formed and 60 % of the organic content of the film was lost. In order to investigate if the organic products expected from the film, in this initial reaction, were the same as those produced during the decomposition of the intermediate, we collected mass spectra at two different extents of reaction. The first mass spectrum was obtained to detect the organic products associated with the photolysis of the precursor film. The second mass spectrum was

obtained to detect the organic products associated with the photolysis with the intermediate film.

In order to get the photoreaction times to independently measure the organic products of equations 3-1 and 3-2, a $Mn(O_2CCH(C_2H_5)C_4H_9)_2$ film was prepared on a silicon chip. The photochemical reaction of the film was carried out with the irradiation of an Oriel spectral calibration UV lamp and monitored by FTIR. It was found that during the first 30 min irradiation, the intermediate FTIR absorption band at 1550 cm^{-1} appeared and reached the maximum and the rest of the FTIR absorption bands decreased. This indicated that the $Mn(O_2CCH(C_2H_5)C_4H_9)_2$ precursor film had decomposed and that the intermediate had been formed.

It was also found that it took a further 12 hr photolysis for the intermediate absorption band at 1550 cm^{-1} to decrease to 70 % its maximal intensity. This indicated that the intermediate had undergone substantial reaction. When the film was irradiated using the UV lamp for 15 hr, all the FTIR bands decreased to the baseline, which indicated that the intermediate had decomposed completely.

The MS samples were then prepared. A $Mn(O_2CCH(C_2H_5)C_4H_9)_2$ film on a silicon chip was prepared by spin coating from $Mn(O_2CCH(C_2H_5)C_4H_9)_2$ in mineral spirits solution. The sample in a vacuum chamber was irradiated using an UV lamp for 20 min. Based on the above results, we expected the products obtained at this point are associated with the conversion of the original precursor to the intermediate. The gas phase was introduced into the mass spectrometer. The mass spectral data are presented in Table 3-2.

The spectrum had peaks at m/e of 100, 98, 85, 84, 71, 70, 57, 56 and 43. The peaks at m/e of 100, 85, 71, 57 and 43 are associated with heptane (C_7H_{16}, m/e=100) and its

44

fragments, $C_6H_{13}{}^+$(m/e=85); $C_5H_{11}{}^+$(m/e=71); $C_4H_9{}^-$(m/e=57); $C_3H_7{}^+$(m/e=43). The

peaks at m/e of 98, 84, 70 and 56 are associated with heptene (C_7H_{14}, m/e=98) and its

fragments, C_6H_{12}(m/e=84); C_5H_{10}(m/e=70); C_4H_8(m/e=56). A peak at m/e of 44, which

corresponded to carbon dioxide, was also detected. This result suggested that the

photolysis of the precursor film produced heptane, heptene and carbon dioxide. Table 3-

2 summaries the data and interpretation[18, 19] of the mass spectrum of the volatile products

from photolysis of the $Mn(O_2CCH(C_2H_5)C_4H_9)_2$ film.

The photochemical reaction of the precursor film described in equation 3-3 is

consistent with the results.

$$2\ Mn(O_2CCH(C_2H_5)C_4H_9)_2 \xrightarrow{\ h\nu\ } Mn(O_2CCH(C_2H_5)C_4H_9)_x$$
$$+\ Mn + 2\ CO_2 + C_7H_{16} + C_7H_{14} \qquad (3\text{-}3)$$
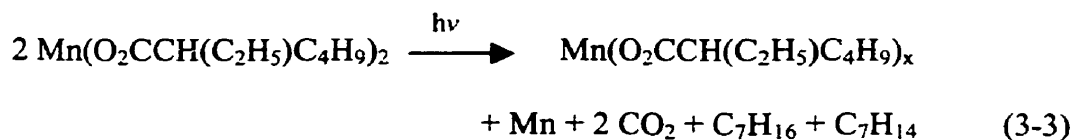
A second $Mn(O_2CCH(C_2H_5)C_4H_9)_2$ film on a silicon chip was prepared by spin

coating from $Mn(O_2CCH(C_2H_5)C_4H_9)_2$ in mineral spirits solution again. The sample was

irradiated using the UV lamp for 30 min. At this reaction extent, the precursor film had

reacted and intermediate had been formed. The intermediate film was then irradiated for

12 hr in a vacuum chamber. This allowed us to collect the volatile products associated

with the reaction of the intermediate. The gas phase in the vacuum chamber was

introduced into the mass spectrometer. The mass spectrum detected the volatile organic

products from the intermediate.

Table 3-2 The MS result of starting precursor and intermediate

Photolysis of	m/e	Assignment
Precursor film	100, 85, 71, 57, 43	C_7H_{16} (heptane)
	98, 84, 70, 56	C_7H_{14} (2 or 3-heptene)
	44	CO_2
Intermediate film	100, 85, 71, 57, 43	C_7H_{16} (heptane)
	98, 84, 70, 56	C_7H_{14} (2 or 3-heptene)
	44	CO_2

The spectrum had peaks at m/e of 100, 98, 85, 84, 71, 70, 57, 56 and 43. The peaks at

m/e of 100, 85, 71, 57 and 43 are associated with heptane (C_7H_{16}, m/e=100) and its

fragments, $C_6H_{13}{}^+$(m/e=85); $C_5H_{11}{}^+$(m/e=71); $C_4H_9{}^+$(m/e=57); $C_3H_7{}^+$(m/e=43). The

peaks at m/e of 98, 84, 70 and 56 are associated with heptene (C_7H_{14}, m/e=98) and its

fragments, C_6H_{12}(m/e=84); C_5H_{10}(m/e=70); C_4H_8(m/e=56). A peak at m/e of 44, which

corresponded to carbon dioxide, was also detected. The intermediate produced heptane,

heptene and carbon dioxide upon photolysis. Table 3-2 summaries the data and

interpretation[18,19] of the mass spectrum of the volatile products from photolysis of the

intermediate.

It is found that photolysis of the precursor film and the intermediate film produced the

same organic products. This result confirmed that the intermediate has the same ligands

as starting material. The equation 3-4 is a proposed photochemical reaction of the

intermediate film. The final step in the analysis is to determine the extent of oxidation of the manganese remaining in the film.

$$Mn(O_2CCH(C_2H_5)C_4H_9)_x \xrightarrow{\quad h\nu \quad} Mn + 2\ CO_2 + C_7H_{16} + C_7H_{14} \qquad (3\text{-}4)$$

3.2.4 Auger electron analyses of films produced by the photolysis of

$\quad\quad Mn(O_2CCH(C_2H_5)C_4H_9)_2$

In order to determine elemental composition of the photoproduced film, Auger electron spectroscopy was employed. A film of $Mn(O_2CCH(C_2H_5)C_4H_9)_2$ on silicon chip was prepared by spin coating from $Mn(O_2CCH(C_2H_5)C_4H_9)_2$ in mineral spirits solution. The film was photolysed until no bands from 2-ethylhexanoate ligand were observed in the FTIR spectrum. This indicated that all the ligands were ejected from surface. Argon ion sputtering for 15 seconds cleaned the surface of the photoproduced film. An Auger electron spectrum was obtained.

Figure 3-6 a) presents Auger electron spectrum of the film prepared above. Peaks at 540, 589, 630 eV correspond to manganese (LMM) and a peak at 502 eV is assigned to oxygen (KLL). There is also a peak at 271 eV, which associated with carbon (KLL),[20] originating presumably from the atmosphere. In order to determine the composition of the film, another Auger electron spectrum was obtained after further 15 seconds argon sputtering. It is shown in Figure 3-6 b). The spectrum shows the peaks at 540, 589, 630 eV corresponding to manganese (LMM) and a peak at 502 eV corresponding to oxygen (KLL). No other peak was observed. This confirmed that the film contained only manganese and oxygen.

Table 3-2 lists the sputter time, peak intensity (peak to peak Auger amplitude), sensitivity factor and concentration of manganese, oxygen and carbon. It also includes the composition of the film obtained from the experiment. The calculated compositions were based on the intensity of the manganese signal at 589 eV, the oxygen signal at 502 eV and the carbon signal at 271 eV. The calculated composition of the film presented in Table 3-3 was approximate due to the 30% error of the AES from the sensitivity factor. The composition of the film was within error of MnO, the most stable form of manganese oxide.[21] The reported results of Blair[9] are within experimental error of those determined here.

From the equation 3-3 and 3-4, it was found that photolysis of $Mn(O_2CCH(C_2H_5)C_4H_9)_2$ precursor film resulted in the formation of manganese which reacted with O_2 in the air to produce a MnO film (Equation 3-5).

$$Mn + \frac{1}{2} O_2 \text{ (in air)} \longrightarrow MnO \qquad (3\text{-}5)$$
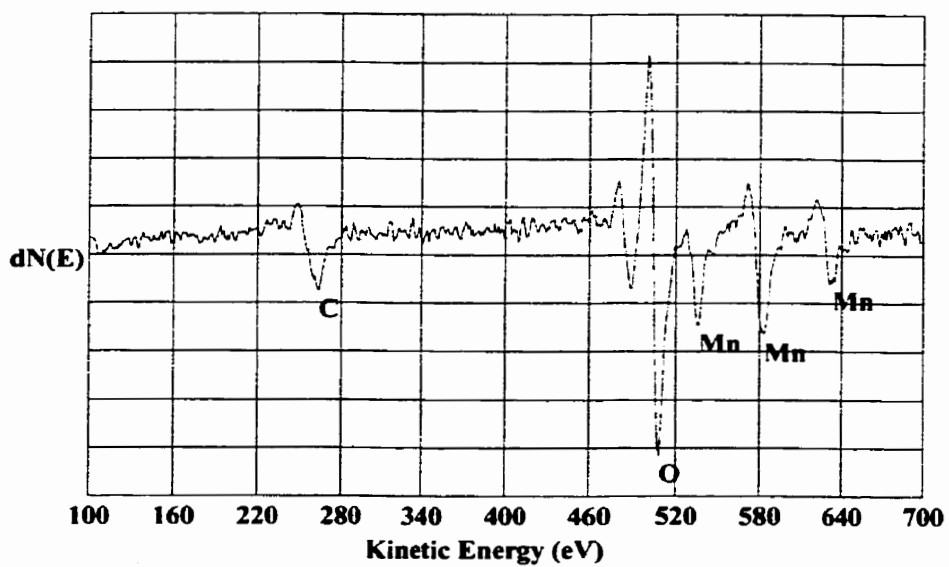
a) Argon ion sputtering for 15 second
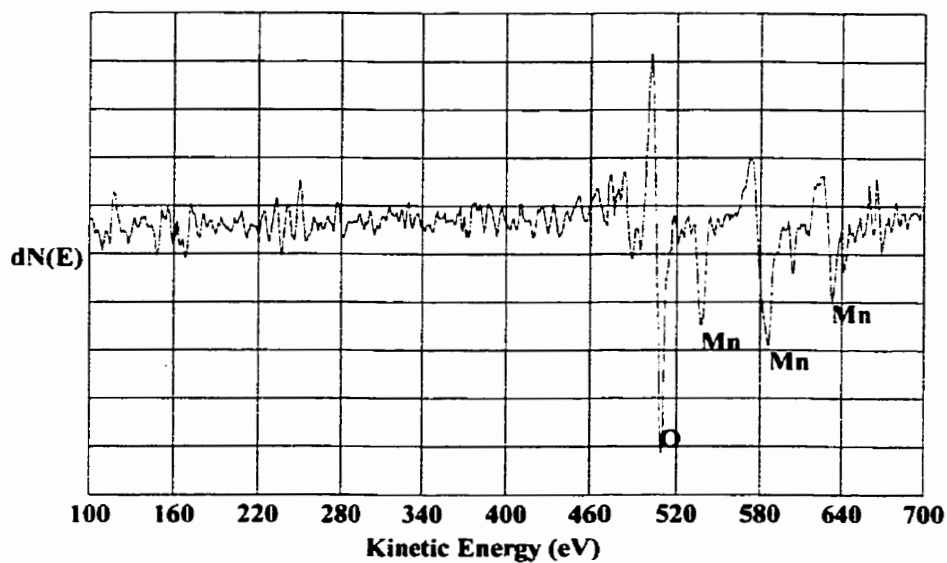
b) Argon ion sputtering for 30 second

Figure 3-6 Auger electron spectra of resultant film from $Mn(O_2CCH(C_2H_5)C_4H_9)_2$

Table 3-3 Auger analysis of resultant film from $Mn(O_2CCH(C_2H_5)C_4H_9)_2$ photolysis

Sputter time (sec)	Relative intensity Mn O C			Sensitivity factor Mn O C			Concentration Mn O C (%)			Composit- ion (calculated)
15	20.2±4	53.5±4	11.8±4	0.25	0.51	0.215	34±7	44±3	22±8	Mn_7O_9
30	25 ±5	53.2±5	0	0.25	0.51	0.215	49±10	51±5	0	MnO

3.2.5 X-ray diffraction from the film produced by the photolysis of
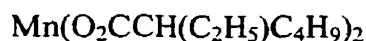
$Mn(O_2CCH(C_2H_5)C_4H_9)_2$

From Auger electron analysis result (see section3.2.4), it was found that the photolysis of the $Mn(O_2CCH(C_2H_5)C_4H_9)_2$ precursor film produced MnO. In this section, X-ray powder diffraction was used to further study the resultant film. Figure 3-7 shows the diffraction spectrum of the film. The peak at $2\theta = 33°$ and $56°$ were from substrate. No peak from the film was observed. This clearly indicated that the photoproduced film was amorphous.

Equation 3-6 shows the result.

$$Mn + \frac{1}{2} O_2 \text{ (in air)} \longrightarrow MnO \text{ (amorphous)} \qquad (3-6)$$
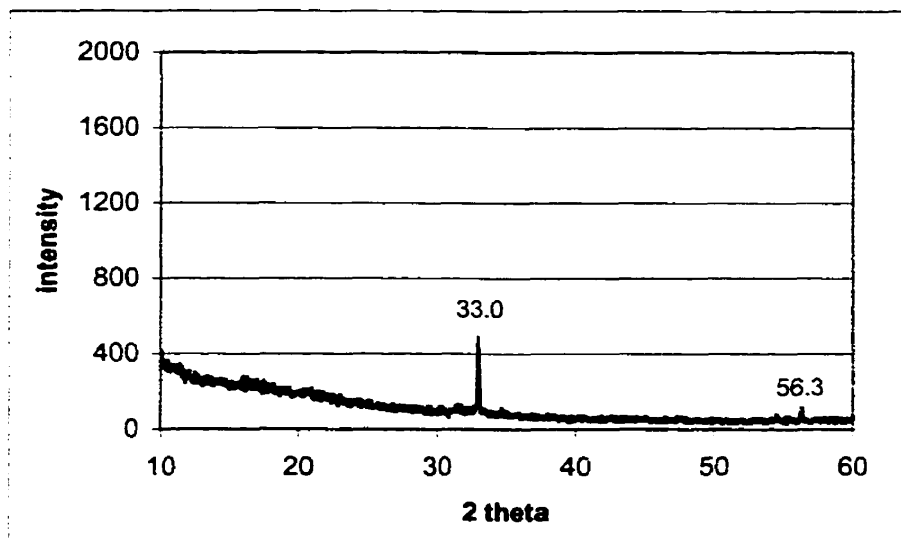
Figure 3-7 X-ray powder diffraction spectrum of photoproduced film from

$Mn(O_2CCH(C_2H_5)C_4H_9)_2$

X-ray powder diffraction was also used to identify the structure of heated film.

The amorphous film on the silicon chip was heated at 600 °C for 6 hr. Figure 3-8 shows

the X-ray powder diffraction spectrum collected from the heated manganese oxide film.

There are peaks at approximately $2\theta = 33$ °, 38 °, 45 °, 49 °, 55 °, 66 ° and 69°. They

correspond to the reflections from α-Mn_2O_3 at (222), (400), (332), (431), (440), (622) and

(444) planes, respectively.[31] These data clearly indicated that amorphous film was

oxidized and crystallized to yield a polycrystalline film of α-Mn_2O_3 upon heating.
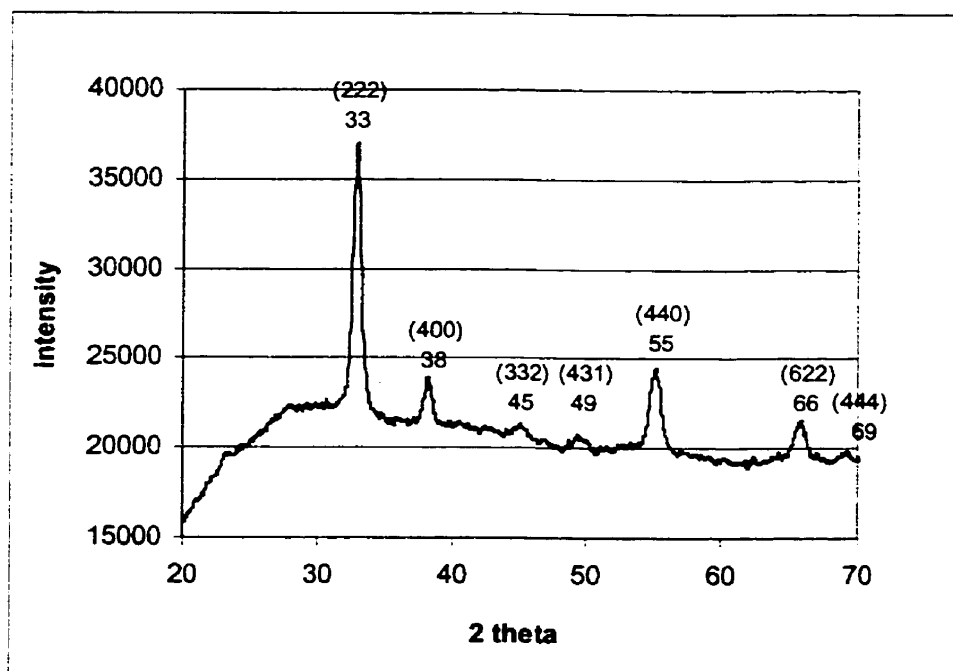
Figure 3-8 X-ray powder diffraction spectrum collected on manganese oxide film after thermal treatment

Auger electron analysis result showed that photolysis of a $Mn(O_2CCH(C_2H_5)C_4H_9)_2$ precursor film resulted in a MnO film on the substrate. During the heating process, MnO reacted with O_2 in the air and crystallized forming α-Mn_2O_3 film.[21] Equation 3-7 is consistent with the result.

$$2 \text{ MnO (amorphous)} + \tfrac{1}{2} O_2 \text{ (in air)} \xrightarrow{600°C} \alpha\text{-}Mn_2O_3 \text{ (polycrystalline)} \qquad (3\text{-}7)$$
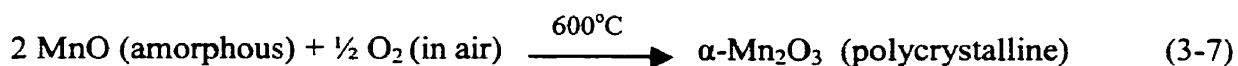
The α-Mn_2O_3 structure is related to that of CaF_2, from which it may be derived by removing one-quarter of the anions and then rearranging the atoms somewhat. The 6-coordinated Mn atoms are of two types. Instead of 8 neighbours at the vertices of a cube,

two are missing. For one-quarter of the Mn atoms these two are at the ends of a body-diagonal, and for the remainder at the ends of a face-diagonal.[32]

3.3 Discussion

The FTIR spectra showed that the Δv value is 125 cm^{-1} for precursor film $Mn(O_2CCH(C_2H_5)C_4H_9)_2$. This value suggested that the bonding of carboxylates with metals is bridging type (Figure 3-3). The FTIR spectra also showed the absorption band at 1693 cm^{-1}. This suggested that the coordinated 2-ethylhexanoic acid exists in the precursor film (Figure 3-4).

From the information above, it is most likely that the $Mn(O_2CCH(C_2H_5)C_4H_9)_2$ film contains chains and clusters held together by the bonding modes shown in Figures 3-3 and 3-4. The combination of these two bonding modes has been established in several molecular structures.[33-37] It is impossible to determine from the data that the film is composed of a single molecule.

It has been shown from FTIR spectroscopy that the photolysis of a $Mn(O_2CCH(C_2H_5)C_4H_9)_2$ precursor film yielded a thermal stable intermediate. The mass spectrum indicated that the volatile photoproducts from $Mn(O_2CCH(C_2H_5)C_4H_9)_2$ were heptane, heptene and carbon dioxide.

Equation 3-8 is consistent with the above result. For convenience, one kind of bonding mode of the precursor molecule is shown in the equation.

$$\text{(structure)} \xrightarrow{h\nu} \text{Intermediate} + Mn + CO_2 + C_7H_{16} + C_7H_{14} \quad (3\text{-}8)$$
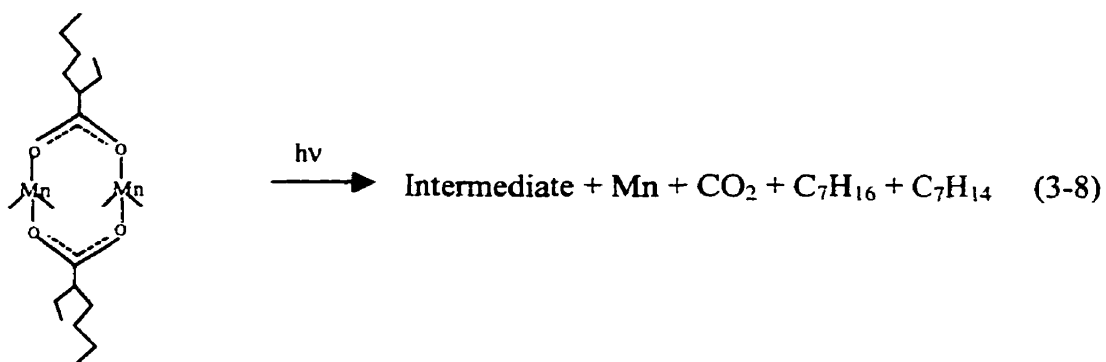
The intermediate produced from the photolysis of the precursor had an FTIR

absorption band at 1550 cm^{-1}. When the absorption band at 1550 cm^{-1} increased to

maximum, the C-H vibrations at 2961 cm^{-1} and $v_s(CO_2)$ bands at 1464 and 1411 cm^{-1}

decreased to roughly 60% of the original absorbance. This suggested that when the

intermediate formed, almost one half of the 2-ethylhexanoate ligand was lost from

$Mn(O_2CCH(C_2H_5)C_4H_9)_2$ precursor.

The FTIR spectra also showed that the Δv value is 86 cm^{-1} for the intermediate. The

value indicated that the bonding of carboxylates with metals of the intermediate is

bidentate type (Figure 3-5).

The mass spectrum indicated that the volatile photoproducts from the intermediate

were heptane, heptene and carbon dioxide. The volatile products produced from the

photolysis of the intermediate are the same as the products produced from the photolysis

of the precursor film. These results confirmed that the intermediate contained the 2-

ethylhexanoate ligand.

Equation 3-9 is a representation of the reaction of the intermediate film.
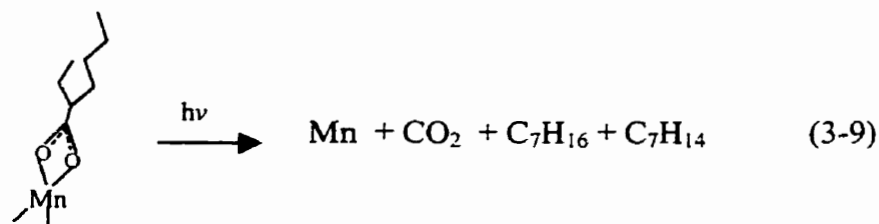
$$\text{(structure)} \xrightarrow{h\nu} \text{Mn} + CO_2 + C_7H_{16} + C_7H_{14} \qquad (3\text{-}9)$$

Auger electron spectroscopy indicated that the photolysis of the $Mn(O_2CCH(C_2H_5)C_4H_9)_2$ precursor film generated MnO as the film remaining on the silicon chip. The manganese oxide film is presumably formed by the reaction of manganese with oxygen in the air.

$$\text{Mn} + \tfrac{1}{2} O_2 \text{ (in air)} \longrightarrow MnO \qquad (3\text{-}10)$$

X-ray powder diffraction indicated that the film remaining on the silicon chip was amorphous. X-ray powder diffraction also indicated that the amorphous MnO film was oxidized and crystallized to yield $\alpha\text{-}Mn_2O_3$ upon heating in air.

$$MnO \text{ (amorphous)} + \tfrac{1}{2} O_2 \text{ (in air)} \xrightarrow{600^\circ C} \alpha\text{-}Mn_2O_3 \text{ (polycrystalline)} \quad (3\text{-}11)$$
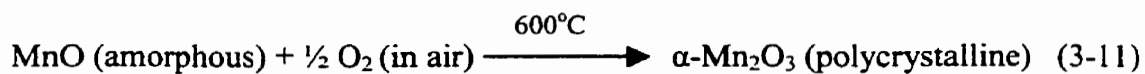
The mechanism of the photoreaction of the $Mn(O_2CCH(C_2H_5)C_4H_9)_2$ film forming Mn, proposed in Figure 3-9, is consistent with all these results. The mechanism proposed
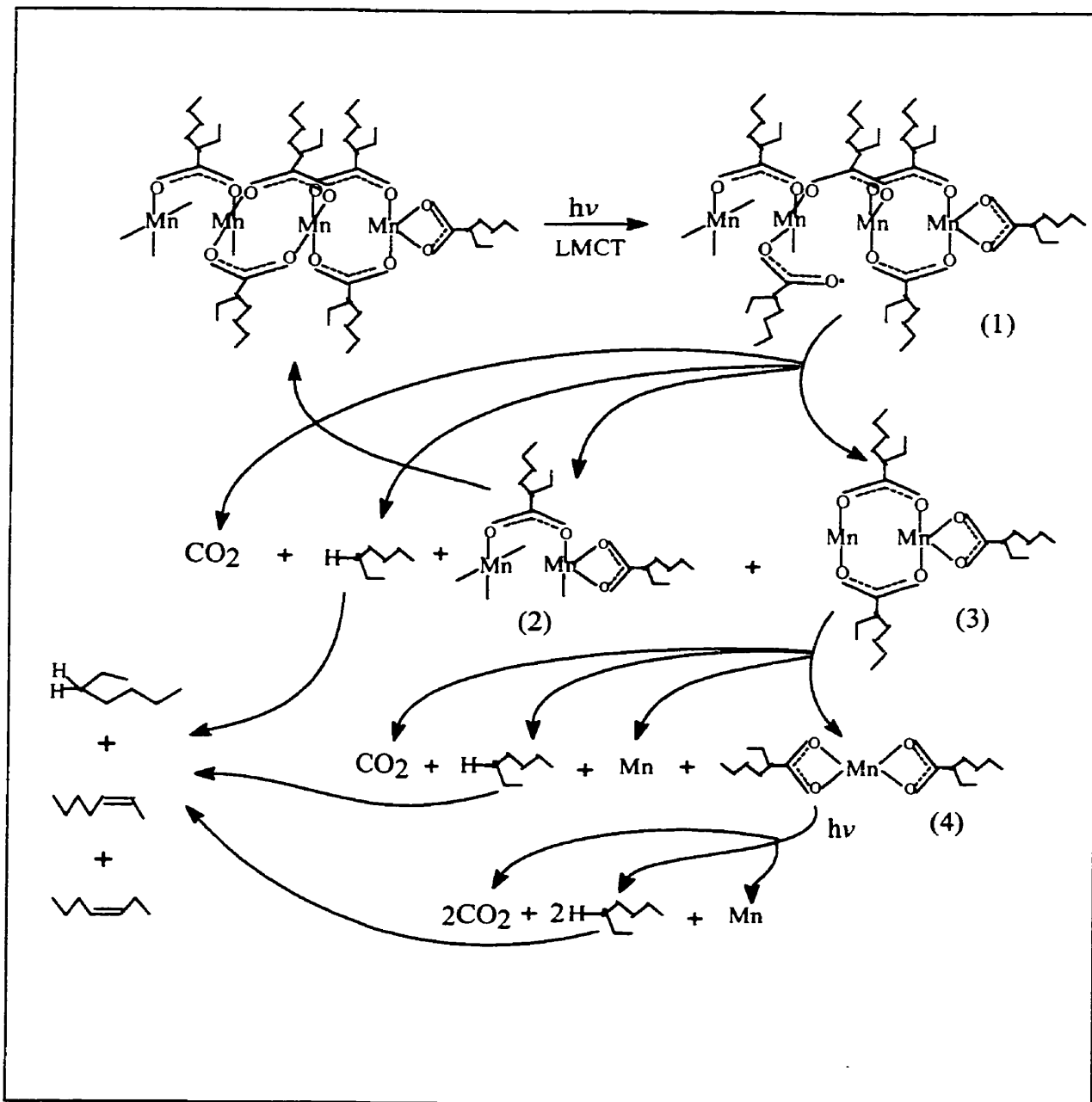
Figure 3-9 Mechanism of the photoreaction of $Mn(O_2CCH(C_2H_5)C_4H_9)_2$ film

56

here is similar to that of the copper carboxylate[38] and cerium carboxylate complexes.[39]

The mechanism in Figure 3-9 is illustrated for the monomer species of $Mn(O_2CCH(C_2H_5)C_4H_9)_2$, because the same photochmistry is expected to be present in monomer units of the cluster. In Figure 3-9, Mn (II) in precursor is indicated as 4 coordination to best represents the oxidation state. However, from X-ray structures we expect coordination number of 6 due to coordinate bonds from lone pairs on oxygen.

The precursor $Mn(O_2CCH(C_2H_5)C_4H_9)_2$ upon absorption of a photon undergoes a ligand to metal charge transfer (LMCT). The transition results in cleaving manganese oxygen bonds in the carboxylate ligand and forming a manganese complex (1). The manganese complex (1) is unstable. One of the manganese oxygen bonds on the same Mn then cleaves, generating 3-heptyl radical, CO_2, species (2) and (3). Species (2) is similar molecule to precursor except that it has shorter chain than precursor because of the cleaving of species (3). It undergoes further photoreaction upon absorption of a photon.

Species (3) is unstable as it contains the reactive Mn(I). It undergoes fragmentation and rearrangement, generating intermediate (4), 3-heptyl radical, CO_2 and Mn. However, the intermediate (4) is thermally stable but photosensitive, undergoing fragmentation upon further irradiation. The fragmentation presumably occurs in a multistage process. Mn, CO_2 and 3-heptyl radicals are formed. The organic radical formed from the precursor and the intermediate undergoes a disproportionation reaction. In this reaction a hydrogen atom is transferred, yielding one equivalent each of heptane and heptene.

The coordinated 2-ethylhexanoic acid in the precursor film is also reactive as a result of a ligand to metal charge transfer (LMCT) upon absorption of a photon. The transition

results in cleaving manganese oxygen bonds in the carboxylate ligand. The 2-ethylhexanoic acid ligand leaves the cluster, forming CO_2 and heptane.

3.4 Conclusion

The photochemical deposition of manganese oxide films from thin films of a $Mn(O_2CCH(C_2H_5)C_4H_9)_2$ precursor has been demonstrated. The photochemistry of $Mn(O_2CCH(C_2H_5)C_4H_9)_2$ has been studied by FTIR, MS and Auger electron spectroscopy.

The $Mn(O_2CCH(C_2H_5)C_4H_9)_2$ precursor film absorbs photons upon UV irradiation undergoing a ligand-to-metal charge transfer transition. This transition finally leads to manganese, C_7H_{16}, C_7H_{14} and CO_2. The manganese reacts with O_2 in air to form amorphous films of manganese oxide on the silicon chip. Upon heating the amorphous manganese oxide films, α-Mn_2O_3 was produced.

3.5 Experimental section

3.5.1 Preparation and photolysis of $Mn(O_2CCH(C_2H_5)C_4H_9)_2$ films

The FTIR spectrophotometer, mass spectrometer and Auger electron spectroscope used in these studies were similar to those introduced in section 2.5.1.

The photolysis beam for the experiment was from a UVP Inc. Model UVG-54 short wave UV-254nm lamp except in section 3.5.2. The photolysis beam in section 3.5.2 was from an Oriel spectral calibration UV lamp.

X-ray diffraction spectrum in Figure 3-7 was obtained using an X-ray generator

system (Model: PW 1730 Philips Electronic Instruments Inc.) with Cu K_α radiation,

Department of Physics, Simon Fraser University. X-ray diffraction spectrum in Figure 3-

8 was obtained using an X-ray generator system (Model: D-max/RAPID-S) produced by

Rigaku.

The $Mn(O_2CCH(C_2H_5)C_4H_9)_2$ sample was obtained commercially from Strem

Chemicals Co. It was obtained as a 40% solution in mineral spirits.

A 0.0615g of the $Mn(O_2CCH(C_2H_5)C_4H_9)_2$ mineral spirits solution was mixed with

0.6150g of hexane. This solution was used as the precursor solution.

An FTIR spectrum of a silicon chip was obtained prior to the film deposition and

used as a reference. The silicon chip was placed on the platform of a spinner. It was

secured on the platform with double-sided tape. A few drops of the precursor solution

prepared were dispensed from a disposable pipette onto a stationary silicon chip, then

accelerated to 2200rpm. The chip was spun until the solvent had evaporated

(approximately 1 min) and a $Mn(O_2CCH(C_2H_5)C_4H_9)_2$ thin film remained on the chip.

An FTIR spectrum of Mn precursor film was obtained. The sample was irradiated

under the UV lamp for 5 min. Another FTIR spectrum was obtained. The extent of the

reaction was monitored by measuring the intensity of the FTIR bands associated with the

complex. This procedure was repeated for accumulated photolysis times of 10, 25 and 45

min at which time no FTIR bands in the region expected for the ligands were observed

(see Figure 3-1 and 3-2).

3.5.2 Mass spectrometric analysis of volatile products produced in the photolysis of $Mn(O_2CCH(C_2H_5)C_4H_9)_2$ films

A mass spectrometer was used to the detection of organic products produced from the photolysis $Mn(O_2CCH(C_2H_5)C_4H_9)_2$ and the organic products from the photolysis of the intermediate (in equation 3-1 and 3-2). The chamber shown in Figure 2-7 was used to collect volatile products from photolysis of films. A sample of $Mn(O_2CCH(C_2H_5)C_4H_9)_2$ in mineral spirits (obtained from Strem Chemicals Co.) was used as the precursor solution. An Oriel spectral calibration UV lamp was used to irradiate the precursor film.

In order to detect organic products, it was necessary to study their photoreaction time. The photoreaction of $Mn(O_2CCH(C_2H_5)C_4H_9)_2$ film was monitored by FTIR. A few drops of this solution were dispensed from a disposable pipette onto a stationary silicon chip, then spun at 2200 rpm. The chip was spun until the solvent had evaporated (approximately 1 min) and a thin film of $Mn(O_2CCH(C_2H_5)C_4H_9)_2$ remained on the chip. An FTIR spectrum of the film was obtained. The sample was then irradiated with the UV lamp in a quartz chamber for 15 min. Another FTIR spectrum was obtained. These procedures were repeated for accumulated photolysis times of 25, 30, 40, 50 min, 1 hr, 1 hr 30 min, 1 hr 45 min, 12 hr and 15 hr at which time FTIR bands associated with the 2-ethylhexanoate ligands were no longer observed.

From the FTIR spectra, it was found that during the first 30 min photolysis, the FTIR bands decreased in intensity. An intermediate band at 1550 cm^{-1} appeared and increased to maximum at 30 min. It indicated that the $Mn(O_2CCH(C_2H_5)C_4H_9)_2$ precursor film had decomposed and the intermediate had been formed during this time. Upon photolysis the film for a further 12 hr, the FTIR band at 1550 cm^{-1} decreased to 70% its maximal

60

intemsity. This indicated that the intermediate had undergone substantial reaction. When the film was irradiated for 15hr, the FTIR bands all decreased to the baseline indicating that all the intermediate decomposed.

A sample for MS was prepared by spin coating $Mn(O_2CCH(C_2H_5)C_4H_9)_2$ precursor solution on a silicon chip at 2200 rpm again. The sample was placed in the bottom part of the quartz chamber. Then, the top and the bottom parts of the device were joined with a greased vacuum o-ring. After evacuation of the chamber by a vacuum pump for an hour, the valve was closed. The sample in the sealed chamber was then irradiated for 20 min with the UV lamp. The chamber with the sample was connected to a mass spectrometer. The mass spectrum of the background was recorded and then the spectrum of the sample was recorded. The spectrum of volatile products was obtained by subtracting that of background from sample spectrum.

Another sample for MS was prepared by spin coating $Mn(O_2CCH(C_2H_5)C_4H_9)_2$ precursor solution on a silicon chip at 2200 rpm again. It was placed in the bottom part of the quartz chamber. The sample was irradiated with the UV lamp for 30 min. Then the top and the bottom parts of the device were joined with a greased vacuum o-ring. After evacuation of the chamber by a vacuum pump for an hour, the valve was closed. The sample in the sealed chamber was then irradiated for 12 hr with the UV lamp. The chamber with the sample was connected to a mass spectrometer again. The mass spectrum of the background was recorded and then the spectrum of the sample was recorded. The MS results are shown in Table 3-2.

3.5.3 Auger analysis of photoproduced film from $Mn(O_2CCH(C_2H_5)C_4H_9)_2$

A Mn(O$_2$CCH(C$_2$H$_5$)C$_4$H$_9$)$_2$ film was prepared as described in section 3.5.2. The film was then irradiated with an UV light for 24 hr. An FTIR of the film was obtained and its spectrum showed that all the bands associated with precursor ligands had been lost. The sample was then moved to the Auger electron spectrometer for analysis. The results are showed in Table 3-3.

3.5.4 Thermal treatment of films produced from Mn(O$_2$CCH(C$_2$H$_5$)C$_4$H$_9$)$_2$

A Mn(O$_2$CCH(C$_2$H$_5$)C$_4$H$_9$)$_2$ film was prepared as described in section 3.5.2. The precursor film was irradiated with an UV lamp for 24 hr. The photoproduced film on the silicon chip was heated in air at 600°C for 6 hr. The X-ray powder diffraction spectrum was obtained. The result is shown in Figure 3-8.

Chapter 4 Fabrication of titanium oxide and manganese oxide multilayer films

4.1 Introduction

In the past several decades multilayer thin films have attracted considerable interest.[40,41] It is hoped that these new materials will exhibit novel and interesting as well as useful properties. Following the study of titanium compound and manganese compound, this chapter will describe the deposition of alternating titanium oxide and manganese oxide multilayer films.

From chapter 2 and chapter 3, it was found that $Ti(i\text{-prop})_2(acac)_2$ and $Mn(O_2CCH(C_2H_5)C_4H_9)_2$ can readily be coated on silicon substrates forming amorphous precursor films. Photolysis of the precursor films in an air atmosphere led to the loss of the ligands. Titanium oxide films and manganese oxide films were obtained on the silicon substrate. Based on these results, it was postulated that a titanium oxide film could be a useful substrate for a $Mn(O_2CCH(C_2H_5)C_4H_9)_2$ precursor film. If it is true, a manganese oxide film could be formed on a titanium oxide film by photolysis of the appropriate precursor film. It was also postulated that a manganese oxide film could be a useful substrate for a $Ti(i\text{-prop})_2(acac)_2$ precursor film. If it is correct, a titanium oxide film could be formed on a manganese oxide film by photolysis of the appropriate precursor film.

The goal of this study was to explore the use of photochemical metal organic deposition (PMOD) to prepare alternating titanium oxide and manganese oxide multilayer films. The new process (PMOD) has some advantages: the reaction is carried

out at room temperature, reaction does not require a sophisticated vacuum chamber as it can be carried out under atmospheric pressure.

The following sections will describe the preparation of multilayer films. The bilayer thickness of the multilayer samples was studied by low angle X-ray powder diffraction. X-ray powder diffraction at high angle was also employed to identify the phase of the multilayer films. Figure 4-1 schematically shows a target multilayer film composed of 9 layers from two different metal oxides on a substrate.
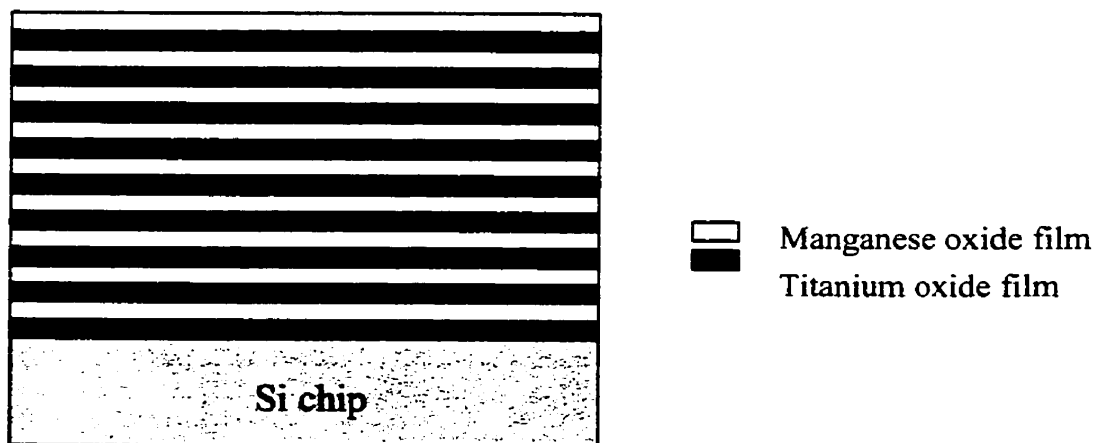
Figure 4-1 Schematic diagram of a target multilayer film composed of alternating 9 layers from titanium oxide and manganese oxide films

4.2 Results

4.2.1 Preparation of alternating titanium and manganese oxides films

A room temperature photochemical method (PMOD) was used for the deposition of titanium oxide/manganese oxide multilayer films. A toluene isopropanol solution of Ti(i-prop)$_2$(acac)$_2$ was used as the precursor solution for the titanium oxide layers. A mineral spirits hexane solution of Mn(O$_2$CCH(C$_2$H$_5$)C$_4$H$_9$)$_2$ was used as the precursor solution for the manganese oxide layers.

Sample ATM was prepared on a 4-inch wafer. The preparation procedure is as follows. A clean silicon wafer was placed on the platform of a spinner. The wafer was secured on the platform by vacuum force. 3 ml of the Ti(i-prop)$_2$(acac)$_2$ stock solution with a precursor to toluene weight ratio of 1:80 was dispensed from a disposable pipette onto the stationary substrate. The substrate was accelerated to 2500 rpm (Figure 4-2a). The wafer was spun until the solvent had evaporated (1 min) and a thin film of precursor remained on the wafer. The wafer with film on the top was removed from the spinner and put on a rotating platform. It was irradiated using UV-254nm light for 30 min on the slowly spinning platform (Figure 4-2b). A control experiment was done to ensure that 30 min irradiation was sufficient to convert the precursor film to an amorphous titanium oxide film.

The wafer was placed on the platform of the spinner again. It was secured on the platform by vacuum force. 3 ml of the Mn(O$_2$CCH(C$_2$H$_5$)C$_4$H$_9$)$_2$ stock solution with a precursor to hexane weight ratio of 1: 160 was dispensed from a disposable pipette onto the stationary substrate. It was then accelerated to 2500 rpm (Figure 4-2c). The wafer with film on the top was removed from the spinner and put on the rotating platform. It

was then irradiated using UV-254nm light for 30 min (Figure 4-2d). A control

experiment was done to ensure that 30 min irradiation was sufficient to convert the

precursor film to an amorphous manganese oxide film.

The procedure was repeated by alternatively spin coating Ti(i-prop)$_2$(acac)$_2$ and

Mn(O$_2$CCH(C$_2$H$_5$)C$_4$H$_9$)$_2$ stock solution and irradiating the coated films until the 9

bilayers were produced.

```
                        ┌──────────────────────────────┐
          ┌────────────▶│     Ti stock solution        │
          │             │  Precursor:toluene = 1:80    │
          │             └──────────────────────────────┘
          │                           │
          │                           ▼
          │                    spin coated              (a)
          │                           │
          │                           ▼
          │                    irradiated               (b)
  ┌───────┴───────┐                   │
  │ 9 repetitions │  (e)              ▼
  └───────────────┘         ┌──────────────────────────────┐
          │                 │     Mn stock solution        │
          │                 │  Precursor:hexane = 1:160    │
          │                 └──────────────────────────────┘
          │                           │
          │                           ▼
          │                    spin coated              (c)
          │                           │
          │                           ▼
          └──────────────────  irradiated               (d)
                                      │
                                      ▼
                      ┌──────────────────────────────┐
                      │ Amorphous films with 9 bilayers │
                      └──────────────────────────────┘
```
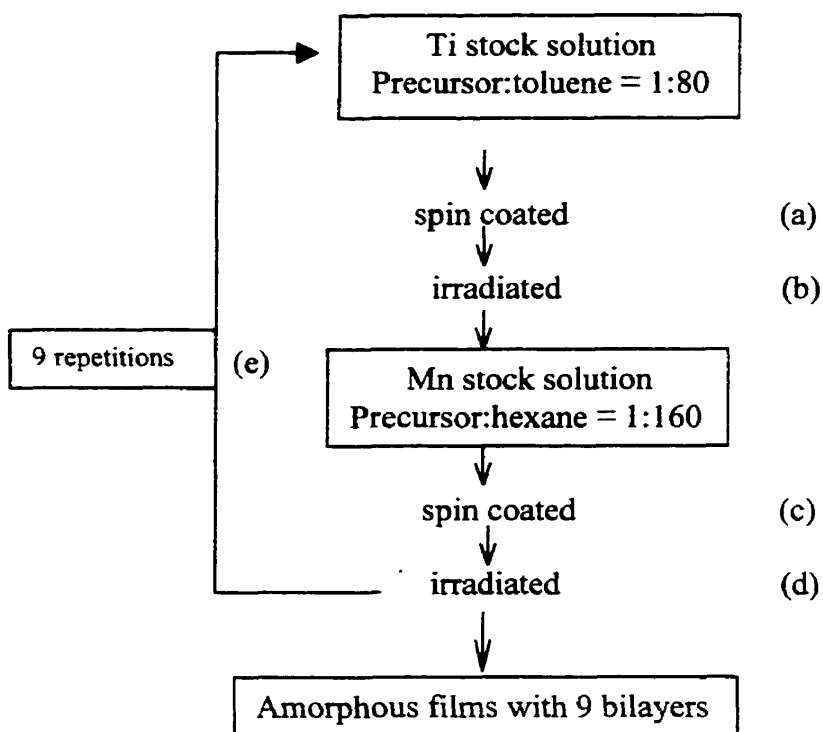
Figure 4-2 Fabrication procedures of multilayer sample (ATM)

Several other samples were prepared by a modification of this procedure. Samples

BTM, CTM, DTM and ETM were prepared on silicon chips of approximate dimensions

10×14mm. The preparation method for these four samples was similar to the method described above. The precursor films of Ti(i-prop)$_2$(acac)$_2$ were prepared by spin coating the stock solutions. They were photolyzed with a UV light without rotation. The precursor films of Mn(O$_2$CCH(C$_2$H$_5$)C$_4$H$_9$)$_2$ were prepared by spin coating the stock solutions. They were photolyzed with a UV light without rotation. The preparation parameters, concentration of precursor solutions, spin speed used for spin coating, photolysis times of the films and the number of layers in each sample, are listed in Table 4-1.

Table 4-1 Preparation conditions of multilayer films

Samples	Ti precursor:toluene (mass ratio)	Mn precursor:hexane (mass ratio)	Spin speed (rpm) Ti	Mn	Photolysis Time (min) Ti	Mn	No.of bilayers	Thickness of bilayer (nm)
ATM	1 : 80	1 : 160	2500	2500	30	30	9	5.3±0.5
BTM	1 : 30	1 : 50	2800	2200	15	15	9	9.1±1.0
CTM	1 : 30	1 : 50	2800	2800	15	15	6	8.6±1.0
DTM	1 : 50	1 : 50	2800	2200	15	15	30	6.8±0.5
ETM	1 : 70	1 : 70	2800	2800	15	15	9	4.6±0.5

4.2.2 Characterization of alternating titanium and manganese oxide films

The 9 bilayer sample ATM was prepared on a 4-inch wafer. The surface of the sample appeared to be optically uniform. It was cut to the approximate dimensions 10×14mm for characterization.

A low angle X-ray diffraction spectrum of the sample was obtained. The X-ray diffraction pattern is shown in Figure 4-3. It reveals apparent periodicity in the multilayer sample. The bilayer thickness is calculated by Bragg equation 4-1, where X-ray wavelength is 0.154 nm. The diffraction peak at $1.67°±0.10°$ indicates that the bilayer thickness of the sample is 5.3±0.5 nm.

$$n\lambda = 2d\sin\theta \qquad 4\text{-}1$$

This material was constructed by nine bilayers so the overall thickness is nine times that of an individual bilayer or 47.7±4.5 nm.
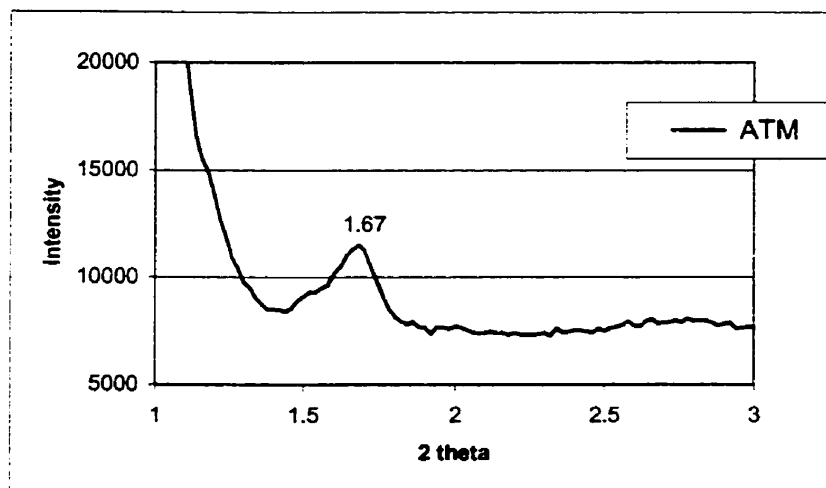
Figure 4-3 Low-angle x-ray diffraction spectrum of 9 layers sample (ATM)

An optical interferometer was also used to measure the overall thickness of the sample ATM. A fringe shift, N, was observed 0.17 ± 0.03. The wavelength of optical interferometer is 546 nm. According to equation 4-2, the sample thickness was 46.4 ± 8.2 nm.

$$T = N * \lambda/2 \qquad\qquad 4\text{-}2$$

The agreement in the thickness obtained from X-ray powder diffraction (47.7 ± 4.5 nm) and optical interferometer (46.4 ± 8.2 nm) is within experimental error.

Figure 4-4 Low angle x-ray diffraction patterns of four samples,

BTM, CTM, DTM and ETM

Figure 4-4 shows the low angle x-ray diffraction patterns of the remaining multilayer samples. It is observed that BTM film has the first order of low angle peak at $0.97°\pm0.10°$ and second order of low angle peak at $1.94°\pm0.10°$. From the Bragg equation, the low angle peaks at $0.97°\pm0.10°$ and $1.94°\pm0.10°$ lead to 9.1 ± 1.0 nm for the bilayer thickness.

It is also observed that CTM film has the first order of low angle peak at $1.02°\pm0.10°$. The bilayer thickness of the film calculated from Bragg equation is 8.6 ± 1.0 nm.

From Figure 4-4, it is found that DTM film has the first order of low angle peak at $1.30°\pm0.10°$. The bilayer thickness of the film calculated from Bragg equation is 6.8 ± 0.5 nm.
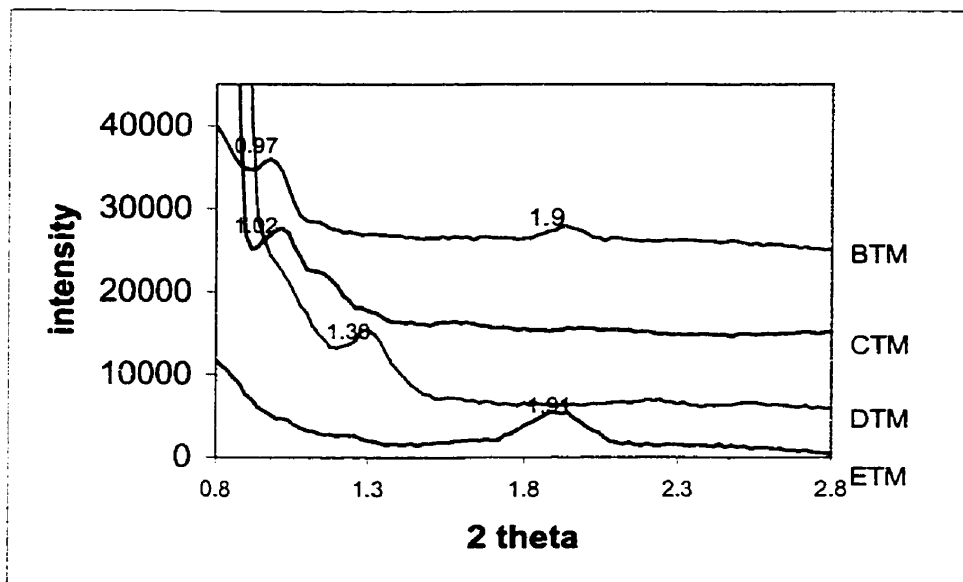
Figure 4-4 also shows that ETM film has the first order reflection of the low angle peak at $1.91°\pm0.10°$, which leads to a bilayer thickness of 4.6 ± 0.5 nm.

From sample BTM to ETM, the first order of low angle peaks shifted to higher angle. It indicates that the bilayer thickness calculated from Bragg equation decrease from sample BTM to ETM. The bilayer thickness of the multialyer samples calculated from low angle XRD are summarized in Table 4-1.

From Table 4-1, it is found that the concentration of precursor solutions of BTM and CTM were same. The spin speed of CTM substrate (2800 rpm) when coating $Mn(O_2CCH(C_2H_5)C_4H_9)_2$ precursor was faster than that of BTM substrate (2200 rpm). It was found that CTM film (8.6 nm) is thinner than BTM film (9.1 nm). This is consistent with the expectation that faster spin speeds of the substrate leads to thinner films.[42]

Comparing sample BTM with DTM, the spin speeds of substrates are same. But the concentration of Ti(i-prop)$_2$(acac)$_2$ for DTM (1:50) is more diluted than for BTM (1:30).

71

As a result, DTM film (6.8 nm) is thinner than BTM film (9.1 nm). This is consistent with the expectation that more diluted precursor solution leads to thinner films.

Comparing sample CTM with ETM, the spin speeds of their substrate were same. The precursors of ETM were more diluted than that of CTM. It was observed that ETM film (4.6 nm) is thinner than CTM film (8.6 nm). This is again consistent with the expectation that more diluted precursor solution leads to thinner films.

The above comparisons showed that diluted precursor solutions and faster spin speeds of substrates produced thinner multilayer samples. This is expected from previous studies of spin coating.[42]

4.2.3 Thermal diffusion in films of alternating titanium and manganese oxides

To explore the structure change of multilayers, low angle x-ray diffraction data were collected as a function of the heating time. The multilayer sample DTM is composed of 30 bilayers of alternating titanium oxide and manganese oxide films. A low angle X-ray diffraction spectrum was obtained from the as-deposited film. XRD spectra were obtained again after it was heated for 1, 2 and 3 hr at 300°C.
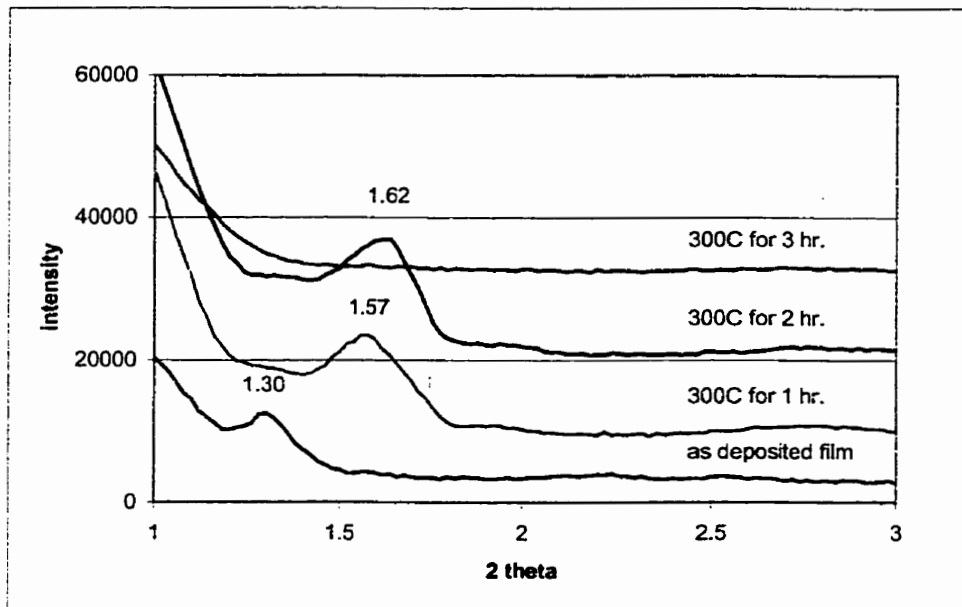
Figure 4-5 Low angle X-ray diffraction patterns of DTM-30 layer film

Figure 4-5 shows the X-ray diffraction patterns of DTM as-deposited film, film heated at 300°C for 1hr, 2hr and 3hr. It is observed that 300 °C heating for 1 and 2 hr leads to a shift of the Bragg reflection to higher angle. This indicates that bilayer thickness of the multilayer film decreased presumably due to the elimination of voids existing in the as-deposited film. The film has become denser. The 300°C heating for 3 hour results in loss of the low-angle peak. This loss suggests that the layered structure does not exist any more because of interdiffusion of the alternating layers.
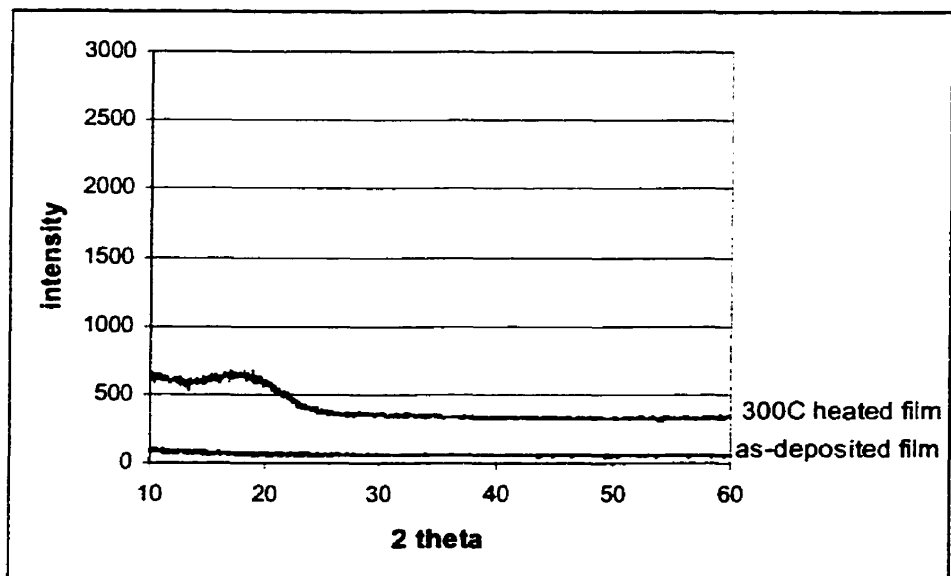
Figure 4-6 High angle XRD spectra collected on DTM sample

In order to characterize multilayer film, high angle XRD spectra were collected on the same sample, DTM. The first high angle XRD spectrum was collected on as-deposited DTM. The second high angle XRD spectrum was collected after it was heated for 3 hr at 300°C. Figure 4-6 shows the XRD spectra. No Bragg diffraction from the as-deposited film and 300°C heated film was observed. This indicated that as-deposited sample, DTM, was amorphous multilayer film. When it was heated for 3 hr at 300°C, it was still amorphous.

4.2.4 Characterization of crystalline films

In order to crystallize the amorphous film, sample DTM was further heated at 700°C

for 3 hr. A high angle XRD spectrum was collected after the sample had been heated.

The spectrum is shown in Figure 4-7. There are peaks at approximately $2\theta = 27°$, 33°, 36

°, 38°, 39°, 41°, 44°, 54° and 57°.
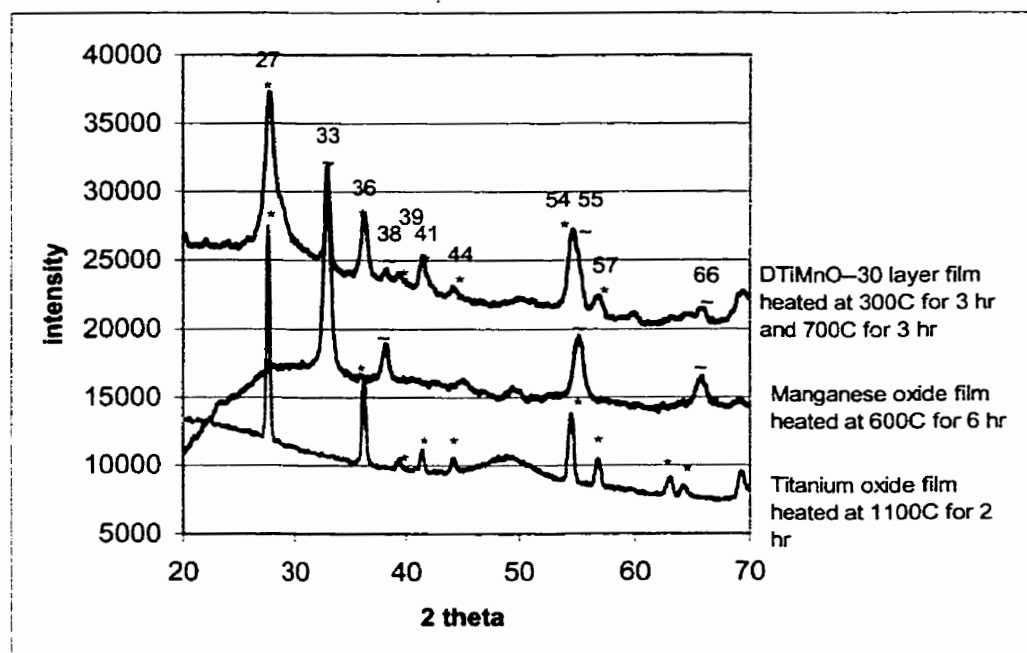
Figure 4-7 High angle XRD spectra of heated 30 layer films DTM, α-Mn_2O_3 (from

Figure 3-7) and TiO_2 films (from Figure 2-5e)

In order to compare with the XRD patterns of possible products, XRD patterns of α-

Mn_2O_3 (produced by the method at chapter 3) and rutile (produced by the method at

chapter 2) are also showed in Figure 4-7.

There are peaks at approximately $2\theta = 27°$, $33°$, $36°$, $38°$, $39°$, $41°$, $44°$, $54°$, $55°$, $57°$, and $66°$ from sample DTM. The peaks at $2\theta = 27°$, $36°$, $39°$, $41°$, $44°$, $54°$ and $57°$ match the peaks from rutile pattern. They correspond to the reflections from the rutile (110), (101), (200), (111), (210), (211) and (220) planes.[23]

The peaks at $2\theta = 33°$, $38°$, $55°$ and $66°$ match the diffraction peaks from a α-Mn_2O_3 sample. They correspond to the reflections from a α-Mn_2O_3 (222), (400), (440) and (622) planes, respectively.[31] The X-ray diffraction pattern suggests that the formation of a α-Mn_2O_3 structure and rutile has occurred in the sample DTM during heating at 700 °C.

Figure 4-8 Phase diagram of MnO_x-TiO_2[43]

Figure 4-8 shows the phase diagram of system MnO_x-TiO_2 in air[43]. H $_{ss}$ = solid

solution $Mn_cTi_{3-c}O_4$ with the hausmannite structure; S $_{ss}$ = solid solution $Mn_xTi_{3-x}O_4$

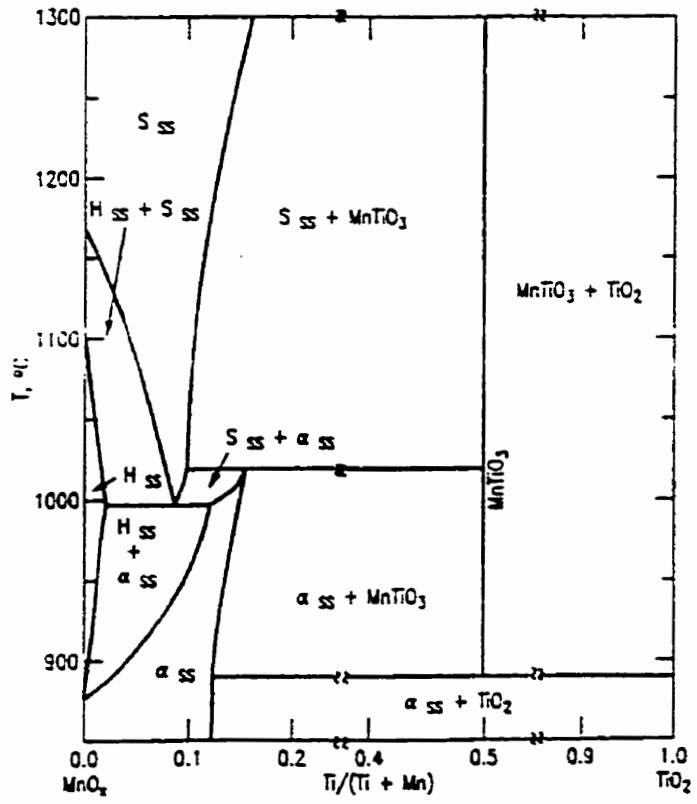with a spinel structure; α $_{ss}$ = solid solution $Mn_pTi_{2-p}O_3$ with α-Mn_2O_3 structure. It is

found that in a Ti/ (Ti + Mn) range of 0.12 ~ 1.0, a solid solution, $Mn_pTi_{2-p}O_3$ with the α-

Mn_2O_3 structure, and titanium dioxide are formed when titanium oxide and manganese

oxide are mixed and heated to 850 °C.

From the preparation parameters in Table 4-1, it was found that the Ti/ (Ti + Mn)

range of sample DTM is in the range of 0.12 ~ 1.0. It is consistent with the phase

diagram that a solid solution of $Mn_pTi_{2-p}O_3$ with the α-Mn_2O_3 structure and titanium

dioxide were formed when it was heated at 700 °C.

The similarity between the XRD result and the expectation from the phase diagram

indicate that the sample may have reached thermodynamic equilibrium. In order to test

whether this is reasonable, we prepared a sample of a non-layered film of titanium and

manganese oxide and subjected it to a similar thermal treatment.

The titanium manganese mixed oxide sample, FTM, was prepared as follow. A 1:1

stoichiometric mixture of Ti(i-prop)$_2$(acac)$_2$ and Mn(O_2CCH(C_2H_5)C_4H_9)$_2$ in isopropanol

mineral spirits was prepared first. The mixture was spin coated onto a silicon substrate.

An FTIR spectrum of the film was obtained. It showed the absorption bands of both

precursors. This film was photolysed with a 254 nm light for 24 hr. Another FTIR

spectrum was obtained which ensured us that all absorption associated with the precursor

ligands had decreased to baseline. The sample was heated at 600°C for 2 hr. An X-ray

powder diffraction pattern was obtained. In order to facilitate a comparison, the XRD

patterns of the multilayer sample, DTM, that had been heated at 700 °C and nonlayered

film, FTM, that had been heated at 600 °C are shown in Figure 4-9.
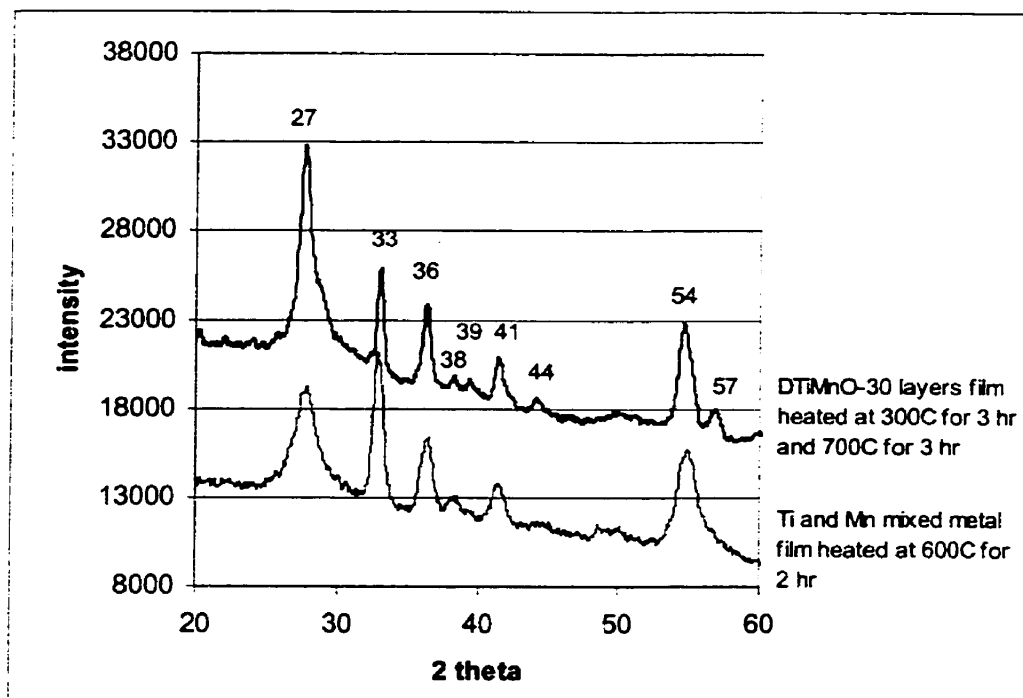
Figure 4-9 High angle XRD spectra of heated films

From Figure 4-9 it is found that there are peaks at approximately $2\theta = 27°$, $33°$, $36°$,

$38°$, $41°$ and $54°$ from sample FTM. As we mentioned earlier, there are peaks at

approximately $2\theta = 27°$, $33°$, $36°$, $38°$, $39°$, $41°$, $44°$, $54°$ and $57°$ from sample DTM.

The X-ray diffraction pattern of non-layered sample FTM is like that of multilayer

sample DTM. It is assumed that the peaks at $2\theta = 39°$, $44°$ and $57°$ for FTM film were

too weak to be detected. The XRD patterns indicated that heating multilayer sample

produced the same products as that of non-layered metal oxide mixture.

The ratio of the Ti/ (Ti + Mn) of sample FTM is 0.5. It is consistent with phase diagram that a solid solution of $Mn_pTi_{2-p}O_3$ with the α-Mn_2O_3 structure and titanium dioxide was formed when the sample FTM was heated at $600^{\circ}C$.

All these results indicated that when the multilayer sample, DTM, was heated at 700 $^{\circ}C$ and the titanium manganese oxide, FTM, was heated at 600 $^{\circ}C$, a solid solution of $Mn_pTi_{2-p}O_3$, with the α-Mn_2O_3 structure, and rutile were formed. These results suggest that they are the thermodynamic products in both cases.

4.3 Discussion

Photochemical metal organic deposition is a room temperature deposition method. By this method, five multilayer samples ATM, BTM, CTM, DTM and ETM have been prepared. The formation of multilayer samples indicated that amorphous titanium oxide film formed a useful substrate for the manganese precursor film. It also indicated that the amorphous manganese oxide film formed a useful substrate for the titanium precursor film. The low angle X-ray data confirmed that each layer remained intact while additional layers were deposited.

The multilayer samples we prepared have different thickness. They were fabricated by adjusting the deposition parameters. The basic variables are concentration of precursor solutions and spin speed of the substrates.

More dilute precursor solutions and faster spin speed of substrate produce thinner multilayer sample. These results are consistent with results found for single layer films.[42] This feature clearly indicated that our PMOD method could not only be used to fabricate multilayer thin films, but also to control the layer thickness of the films. This control is

79

achieved by controlling the spin speed of the silicon substrate and the concentration of the precursor solutions. This feature will permit the tailoring of physical properties of films as a function of compositional layer thickness.

The multilayer samples have been characterized by low angle X-ray diffraction. It was observed that intensity of Bragg reflections in low angle X-ray diffraction spectra were not high. The reason for the low intensity is that Ti and Mn have similar atomic numbers, hence, the contribution of the compositional modulation to the XRD intensity is small.[44] The bilayer thickness of multilayer samples we prepared were 4 ~ 10 nm, as determined by the low angle X-ray diffraction. The X-ray data confirmed that the layer thickness was reproducible.

The X-ray diffraction data have been collected as a function of heating time at 300 °C. The X-ray peaks shifted and then were lost due to the interdiffusion of the layers. In the future, it may be possible to use low angle X-ray diffraction to measure the interdiffusion rates of the multilayer samples.

The samples were also characterized by high angle X-ray diffraction. The results suggested that both multilayer and nonlayered films reached thermodynamic equilibrium after they were heated at 600 ~ 700 °C. The thermodynamic products are the solid solution, $Mn_pTi_{2-p}O_3$ with $\alpha\text{-}Mn_2O_3$ structure, and rutile.

Figure 4-10 is a diagram, which shows the evolution of the multilayer sample DTM upon thermal treatment. The results were consistent with complete interdiffusion of the original layers when it was heated at 300 °C. Thermal treatment at 700 °C resulted in the formation of a crystal film, which composed of solid solution, $Mn_pTi_{2-p}O_3$ with $\alpha\text{-}Mn_2O_3$ structure, and rutile.

Multilayer sample   Nonlayered amorphous film   Crystal film composed of
DTM   solid solution $Mn_pTi_{2-p}O_3$ and rutile
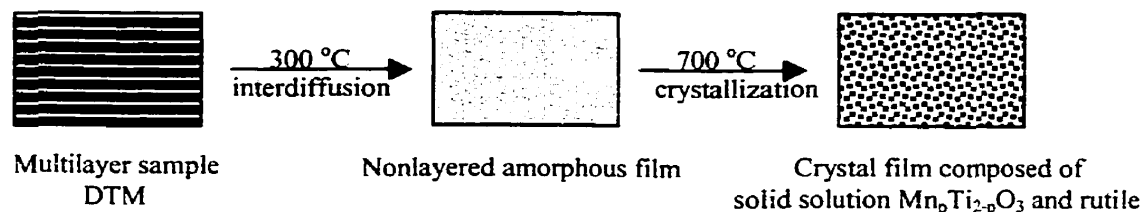
Figure 4-10 A diagram of the multilayer sample structure change by low and high

temperature treatment

The heating rate is a key to control the multilayer structure change. By changing the

heating rate, it allows the fabrication of materials with different structure. As a future

work, it would be useful to heat multilayer samples at different heating rate. It should be

possible to produce a multilayer film, which is composed of solid solution, $Mn_pTi_{2-p}O_3$

with the α-Mn_2O_3 structure, and rutile. This will not be a thermodynamic product, but a

product that is kinetically trapped (Figure 4-11).

Heating at suitable rate

▢ Manganese oxide   ▢ Solid solution $Mn_pTi_{2-p}O_3$
■ titanium oxide   ■ rutile

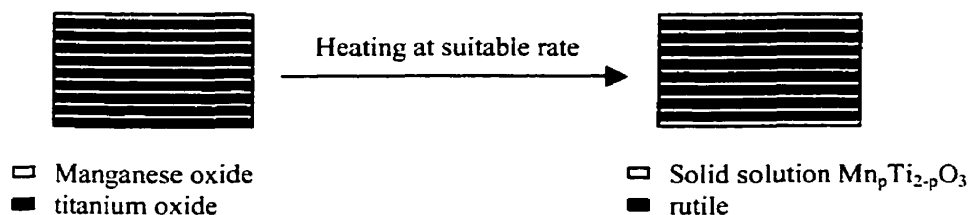Figure 4-11 A diagram of the kinetic product

4.4 Conclusion

Multilayer films composed of titanium oxide and manganese oxide layers have been

fabricated by photochemical metal organic deposition for the first time. The multilayer

structure was confirmed by the observation of Bragg diffraction peaks at small angles.

The ability to control the thickness of the layers by PMOD has been demonstrated. Five

multilayer films with bilayer thickness of 4.6 nm, 5.3 nm, 6.8 nm, 8.6 nm and 9.1 nm were prepared. This thesis has established that this new process is a promising technique for the deposition of metal oxide multilayer films.

4.5 Experimental section

4.5.1 Instruments and materials

N-type Si(100) wafers obtained from Shin Etsu were used as substrates. They were cleaned with acetone before use. A spinner from Laurell Technologies Corp was used to coat films on 4-inch wafers. An in house built spin coater was used to coat films on chips with 10×14mm size. An in house built motor was used to spin a 4-inch wafer during the photolysis.

A $Ti(i\text{-prop})_2(acac)_2$ isopropanol solution, 75%, was obtained from Aldrich Co. The $Mn(O_2CCH(C_2H_5)C_4H_9)_2$ mineral spirits solution, 40%, was obtained from Strem Chemical Co.

The photolysis beam was from a UVP Inc. model UVG-54 short wave UV-254 nm lamp. The FTIR spectra were obtained with 4 cm^{-1} resolution using a Bomem MB-120 FTIR spectrophotometer.

Low angle X-ray diffraction spectra were obtained using an X-ray generator system (Model: PW 1730 Philips Electronic Instruments Inc.) with Cu K_α radiation, Department of Physics, Simon Fraser University.

High angle X-ray diffraction spectra were obtained using an X-ray generator system (Model: D-max/RAPID-S) produced by Rigaku.

4.5.2 Preparation and photolysis of single layer films

In order to find out the photolysis time for each precursor film of multilayer samples, two experiments were conducted. One experiment was performed to obtaine the photolysis time required to convert a Ti(i-prop)$_2$(acac)$_2$ film to titanium oxide. The other one was to obtaine the photolysis time required to convert a Mn(O$_2$CCH(C$_2$H$_5$)C$_4$H$_9$)$_2$ film to manganese oxide.

Ti(i-prop)$_2$(acac)$_2$ precursor solution was prepared by mixing 0.0380g of Ti(i-prop)$_2$(acac)$_2$ complex solution with 1.1493g of toluene (mass ratio 1:30). A few drops of precursor solution were dispensed from a disposable pipette onto a stationary silicon chip with 10x14mm size. The chip was spun at 2500 rpm for 1 min. The film on the chip was irradiated with a 254 nm light. FTIR was obtained every minute to monitor the photoreaction of the film. It was found that after 13 min photolysis, the FTIR bands due to the ligands in the precursor no longer were observed.

Mn(O$_2$CCH(C$_2$H$_5$)C$_4$H$_9$)$_2$ precursor solution was prepared by mixing 0.0436g of Mn(O$_2$CCH(C$_2$H$_5$)C$_4$H$_9$)$_2$ complex solution with 2.1867g of hexane (mass ratio 1:50). A few drops of precursor solution were dispensed from a disposable pipette onto a stationary silicon chip. The chip was spun at 2200 rpm for 1 min. The film on the chip was irradiated with a 254 nm light. FTIR was obtained every minute to monitor the photoreaction of the film. It was found that after 13 min photolysis, the FTIR bands due to the ligands in the precursor no longer were observed.

The rest precursor solutions of multilayer samples have the same concentration or more diluted than the precursor solutions we have tested above (see table 4-1). We

decided to photolyze 15 min for each precursor film during the fabrication of multilayer films.

Because sample ATM was prepared on a 4-in wafer, the UV light could reach half of the wafer. We decided to photolyze the precursor films on a turning motor for 30 min during the fabrication of sample ATM.

4.5.3 Fabrication of titanium oxide and manganese oxide multilayer films

Sample ATM was prepared on a 4-inch wafer. The preparation procedure is as follow. A $Ti(i\text{-prop})_2(acac)_2$ precursor solution of ATM was prepared by mixing 0.2685g of $Ti(i\text{-prop})_2(acac)_2$ complex solution with 21.4818g of toluene (mass ratio 1:80). A $Mn(O_2CCH(C_2H_5)C_4H_9)_2$ precursor solution of ATM was prepared by mixing 0.0986g of $Mn(O_2CCH(C_2H_5)C_4H_9)_2$ complex solution with 15.7775g of hexane (mass ratio 1:160).

A clean silicon wafer was placed on the platform of a spinner. The wafer is secured on the platform by vacuum force. A layer of $Ti(i\text{-prop})_2(acac)_2$ precursor film on the wafer were produced by pipetting 3ml of precursor solution onto a stationary wafer, which was then accelerated to 2500 rpm. The wafer was spun until the solvent had evaporated (1min) and a thin film of precursor remained on the wafer. The wafer with film on the top was removed from the spinner and put on a motor. It was irradiated using UV-254nm light for 30min on the low spin motor. The wafer was placed on the platform of the spinner again. A layer of $Mn(O_2CCH(C_2H_5)C_4H_9)_2$ precursor film was produced by pipetting 3ml of precursor solution onto the stationary wafer, which was then accelerated to 2500 rpm. The wafer with film on the top was removed from the spinner and put on the motor. It was irradiated using UV-254nm light for 30min on the low spin

motor. The procedure was repeated by spin coating Ti(i-prop)$_2$(acac)$_2$ and

Mn(O$_2$CCH(C$_2$H$_5$)C$_4$H$_9$)$_2$ stock solutions and irradiating precursor films until the 9

bilayers were achieved.

The method of preparing BTM, CTM, DTM and ETM is similar. All these samples

were prepared on silicon chips with 10x14mm size. Their preparation parameters, such

as spin speed, photolysis time and the number of bilayer are showed in Table 4-1.

A Ti(i-prop)$_2$(acac)$_2$ precursor solution of BTM was prepared by mixing 0.0380g of

Ti(i-prop)$_2$(acac)$_2$ complex solution with 1.1493g of toluene (mass ratio 1:30). A

Mn(O$_2$CCH(C$_2$H$_5$)C$_4$H$_9$)$_2$ precursor solution of BTM was prepared by mixing 0.0436g of

Mn(O$_2$CCH(C$_2$H$_5$)C$_4$H$_9$)$_2$ complex solution with 2.1867g of hexane (mass ration 1:50).

A clean silicon chip of 10x14mm was placed on the platform of a spin coater. It was

secured on the platform with double-sided tape. A few drops of Ti(i-prop)$_2$(acac)$_2$

precursor solution were dispensed from a disposable pipette onto the stationary silicon

chip. The chip was spun at 2800 rpm for 1 min. The chip with the film was removed

from the spin coater and irradiated with 254nm light for 15min. The sample chip was

secured on the spin coater again with double-sided tape. A few drops of

Mn(O$_2$CCH(C$_2$H$_5$)C$_4$H$_9$)$_2$ precursor solution were dispensed from a disposable pipette

onto the stationary sample chip. The chip was spun at 2200 rpm for 1 min. The sample

chip was removed from the spin coater and irradiated with a 254 nm light for 15min. The

multilayer sample of ATM was prepared by alternating spin coating from two precursor

solutions on a spin coater and photolysis using a 254 nm light until 9 bilayers were

achieved.

A Ti(i-prop)$_2$(acac)$_2$ precursor solution of CTM was prepared by mixing 0.0329g of

Ti(i-prop)$_2$(acac)$_2$ complex solution with 1.0161g of toluene (mass ratio 1:30). A

Mn(O$_2$CCH(C$_2$H$_5$)C$_4$H$_9$)$_2$ precursor solution of CTM was prepared by mixing 0.0305g of

Mn(O$_2$CCH(C$_2$H$_5$)C$_4$H$_9$)$_2$ complex solution with 1.5112g of hexane (mass ratio 1:50).

The 6 bilayer multilayer sample was prepared by alternating spin coating from two

precursor solutions on a spin coater and photolysis with a 254 nm light.

A Ti(i-prop)$_2$(acac)$_2$ precursor solution of DTM was prepared by mixing 0.0506g of

Ti(i-prop)$_2$(acac)$_2$ complex solution with 2.5301g of toluene (mass ratio 1:50). A

Mn(O$_2$CCH(C$_2$H$_5$)C$_4$H$_9$)$_2$ precursor solution of DTM was prepared by mixing 0.0350g of

Mn(O$_2$CCH(C$_2$H$_5$)C$_4$H$_9$)$_2$ complex solution with 1.7530g of hexane (mass ratio 1:50).

The 30 bilayer multilayer sample was prepared by alternating spin coating from two

precursor solutions on a spin coater and photolysis with a 254 nm light.

A Ti(i-prop)$_2$(acac)$_2$ precursor solution of ETM was prepared by mixing 0.0340g of

Ti(i-prop)$_2$(acac)$_2$ complex solution with 2.3861g of toluene (mass ratio 1:70). A

Mn(O$_2$CCH(C$_2$H$_5$)C$_4$H$_9$)$_2$ precursor solution of ETM was prepared by mixing 0.0339g of

Mn(O$_2$CCH(C$_2$H$_5$)C$_4$H$_9$)$_2$ complex solution with 2.3750g of hexane (mass ratio 1:70).

The 9 bilayer multilayer sample was prepared by alternating spin coating from two

precursor solutions on a spin coater and photolysis with a 254 nm light.

4.5.4 Fabrication of titanium manganese mixed metal oxide film

The precursor solution of titanium manganese mixed metal oxide sample, FTM, was

prepared by mixing 0.0619g of Ti(i-prop)$_2$(acac)$_2$ complex solution with 0.1081g of

Mn(O$_2$CCH(C$_2$H$_5$)C$_4$H$_9$)$_2$ complex solution (molar ration of titanium:manganese=1:1).

A few drops of the precursor solution were dispensed from a disposable pipette onto a stationary chip. The sample chip was spun at 3000 rpm for 1 min. An FTIR was obtained on the sample chip. The sample chip was irradiated with 254 nm light for 24 hr. Another FTIR was obtained. It was found from the FTIR spectra that all absorption associated with the precursor ligands had decreased to baseline.

The sample chip was heated in an atmosphere in an oven at 600°C for 2 hr. A high angle X-ray diffraction pattern was obtained (Figure 4-9).

4.5.5 X-ray analysis of multilayer samples

After multilayer samples of ATM, BTM, CTM, DTM and ETM were prepared. The low angle X-ray diffraction patterns were obtained on the as-deposited films (Figure 4-3 and Figure 4-4).

For sample DTM, a high angle X-ray diffraction spectrum was also obtained from as-deposited sample. The sample was heated in an atmosphere in an oven at 300°C for 1hr. The second low angle XRD was obtained. The sample was heated in the oven at 300°C for another 1 hr. The third low angle XRD was obtained. After the sample was heated in the oven at 300°C for 1 hr again, both low and high XRD were obtained (Figure 4-5, Figure 4-6). The last heating was in the oven at 700°C for 3 hr. Only a high angle XRD was obtained (Figures 4-7 and 4-9)

References

1. B. M. Clemens, *Phys. Rev. B*, **33**, 7615, (1986).

2. T. Hayashi and T. Tanaka, *Jpn. J. Appl. Phys.*, **34**, 5100, (1995).

3. Y. P. Lee, S. K. Kim, J. S. Kang, J. I. Jeong, J. H. Hong, Y. M. Koo and H. J. Shin, *J. Vac. Sci. Technol.*, A **12**(5), 2672, (1994).

4. J. J. Senkevich and S. B. Desu, *Thin Solid Films*, **322**, 148, (1998).

5. R. H. Hill, A. A. Avey, S. L. Blair, M. Gao, B. J. Palmer, *Mater. Chem. and Phys.*, **43**, 233, (1996).

6. S.L. Blair and R.H. Hill, *ACS Symposium Series*, **706**, 53, (1998).

7. Y. M. Shi, G. Z. Li and R. H. Hill, *Mater. Sci. in Semi. Pro.*, **2**, 297, (1999).

8. Anthony R. West, *Solid State Chemistry and its Applications*, Chapman and Hall, London, 4-18, (1995).

9. S. L. Blair, *Photochemical Deposition of Metal and Metal Oxide Films from Amorphous Films of Inorganic Precursors*, Ph.D. thesis, Simon Fraser University, (1996).

10. T. W. Kim, M. Jung, H. J. Kim, T. H. Park, *Appl. Phys. Lett.*, **64**, 1407, (1994).

11. M. Takeuchi, T. Itoh, and H. Nagaska, *Thin Solid Films*, **51**, 83, (1978).

12. K. Okimura, N. Maeda and A. Shibata, *Thin Solid Films*, **281-282**, 427, (1996).

13. N. Martin, C. Rousselot and D. Rondot etc., *Thin Solid Films*, **300**, 113, (1997).

14. K. S. Yeung and Y. W. Lam, *Thin Solid Films*, **109**, 169, (1983).

15. K. Nakamoto, *Infrared and Raman Spectra of Inorganic and Coordination Compounds*, Fourth edition, New York; John Wiley and Sons (1986).

16. D. C. Bradley and C.E. Holloway, *J. Chem. Soc.*, (A) 282, (1969).

17. D. C. Bradley and R. C. Mehrotra, *Metal Alkoxides*, Academic Press Inc. London, 116, (1978).

18. Fred W. Mclafferty, *Interpretation of Mass Spectra*, Fourth edition, Mill Valley, California, University Science Books (1993).

19. S. R. Heller, G. W. A. Milne and L. H. Gevantman, *EPA/NIH Mass Spectral Data Base*, U. S. Government Printing Office, Washington, 35, 83, 3980, 75, 5283, (1978).

20. L. E. Davis, N. C. MacDonald, P. W. Palmberg, G. E. Riach, R. E. Weber, *Handbook of Auger Electron Spectroscopy*, Second edition, Physical Electronics Division Perkin-Elmer Corporation, Minnesota.

21. F. Albert Cotton and Geoffrey Wilkinson, *Advanced Inorganic Chemistry*, Sixth edition, John Wiley & Sons, New York, (1999)

22. JCPDS-ICDD, file numbers 21-1272.

23. JCPDS-ICDD, file numbers 21-1276.

24. Rao, C. N. R., *Transition Metal Oxides*, Washington, 14, (1974).

25. M. Gao and R. H. Hill, *J. Photochem. and Photobio. A: Chem.*, **97**, 73, (1996).

26. M. Isai, K. Yamaguchi, H. Iyoda, H. Fujiyasu, *J. Mater. Res.*, **14**, 1653, (1999).

27. C. H. Hare and M. G. Fernald, *Modern Paint Coat*, **74**, 40, (1984).

28. S. C. Pang and M. A. Anderson, *J. Mater. Res.*, **15**, 2096, (2000).

29. H. J. Emeleus, A. G. Sharpe, *Advances in Inorganic Chemistry and Radiochemistry*, 343, New York San Francisco London, (1977).

30. J. E. Tackett, *Appl. Spectrosc.*, **43**, 483, (1989).

31. JCPD-ICDD, file numbers 41-1442.

32. A. F. Wells, *Structural Inorganic Chemistry*, 545, Fifth edition, Clarendon Express,Oxford, (1984).

33. A. R. E. Baikie, A. J. Howes, M. B. Hursthouse, A. B. Quick, P. Thornton, *Chem. Commun.*, 1587, (1986).

34. R. J. Kulawiec, R. H. Crabtree, G. W. Brudvig, G. K. Schylte, *Inorg. Chem.*, **27**,1309, (1988).

35. S. B. Yu, S. J. Lippard, I. Shweky, A. Bino, *Inorg. Chem.*, **31**, 3502, (1992).

36. M. Murrie, S. Parsons, R. E. P. Winpenny, *J. Chem. Soc., Dalton Trans.*, 1423, (1998).

37. T. S. Yaukey, O. W. Steward, S. C. Chang, *Acta Crystallogr.*, *C*. **54**, 1081, (1998).

38. A. A. Avey and R. H. Hill, *J. Am. Chem. Soc.* **118**, 237, (1996).

39. W. L. Law and R. H. Hill, *Mater. Res. Bull.*, **33**, 69, (1998).

40. M. Nagakubo, T. Yamamoto, M. Naoe, *Mat. Res. Soc. Symp. Proc.*, **151**, 29, (1989).

41. S. Noboru, *J. Appl. Phys.*, **59**, 2514, (1986).

42. C.I. Horvath, *Spin Coated Films of Inorganic Complexes and a Study of the Photochemistry of Metal Complexes with Halogen Ligands*, M.Sc. thesis, 30, Simon Fraser University, (1997).

43. Anna E. McHale and Robert S. Roth, *Phase Equilibria Diagrams*, **XI**, Figure 9613, The American Ceramic Society (1996).

44. S. S. Babkair, *Multilayer Ferromagnetic Thin Films*, PhD. Thesis, 208, University of Salford, United Kingdom, (1990).